universität wien

MASTERARBEIT | MASTER'S THESIS

Titel | Title

Carbonate Coating: Layers on modern glacially striated surfaces An investigation from the südlichen Bockkarkees forefield, Großglockner area, Austria

verfasst von | submitted by

Arian Wawra BSc

angestrebter akademischer Grad | in partial fulfilment of the requirements for the degree of

Master of Science (MSc)

Wien | Vienna, 2024

Studienkennzahl lt. Studienblatt | Degree programme code as it appears on the student record sheet:	UA 066 815
Studienrichtung lt. Studienblatt | Degree programme as it appears on the student record sheet:	Masterstudium Erdwissenschaften
Betreut von | Supervisor:	Univ.-Prof. Daniel Le Heron PhD

Statutory declaration

I declare that I have authored this thesis independently, that I have not used other than the declared sources / resources, and that I have explicitly marked all material which has been quoted either literally or by content from the used sources.

……………………. ……………………………….

Date Signature

Abstract

During investigations in the Großglockner area, I found spots of few millimeters-thick mud layers, covering the bedrock at the way to "Oberwalderhütte". These locations had been released from the ice very recently. Due to the different surfaces and irregular distribution, the layers attract attention and were therefore collected for further investigation.

Created thin sections showed a complex stratigraphic architecture of a succession of very thin different layers, which possibly correspond to different seasons, indicating different decomposition of organic material. It reveals previously undescribed sedimentary structures and stratigraphic architectures at the mm-scale.

Age determination of a selected sample indicate a C14 age of 43 000 years BP, with corresponds to the Hengelo interstadial, a warm period interrupting Würm ice age. This result indicates for the biological origin of the laminae.

Keywords: Carbonate coating layers, micro-structure, glacier

Zusammenfassung

Im Großglockner Gebiet fallen immer wieder wenige Millimeter dicke Ablagerungen auf dem anstehenden Festgestein am Wanderweg in Richtung Oberwalderhütte auf. Dieser Bereich wurde erst kürzlich im Rahmen des Gletscherrückganges freigelegt. Die Ablagerungen zeigen unterschiedliche Oberflächenausprägungen und räumlich unregelmäßige Verteilungen, daher wurden sie näher untersucht.

Dünnschliffanalysen zeigten eine komplexe stratigraphische Architektur aus einer Abfolge von sehr dünnen unterschiedlichen Schichten, welche wahrscheinlich dem unterschiedlichen Abbau von organischem Material in verschiedenen Jahreszeiten entsprechen. Man erkennt bis jetzt unbeschriebene, sedimentäre Strukturen im Millimeterbereich.

Die Altersbestimmung einer ausgewählten Probe ergibt ein C14-Alter von 43 000 Jahren. Dieses Alter entspricht der Hengelo Zwischenerwärmung in der Epoche der Würm Eiszeit. Das Ergebnis unterstützt die Annahme des biologischen Ursprungs der Probe.

Schlüsselwörter: Karbonatablagerungen, Mikrostruktur, Gletscher

Table of Contents

1. Introduction

During visiting the Großglockner area, spectacular examples of glacially striated surfaces can be seen which are locally covered by a few millimeters-thick mud layer at higher elevations.

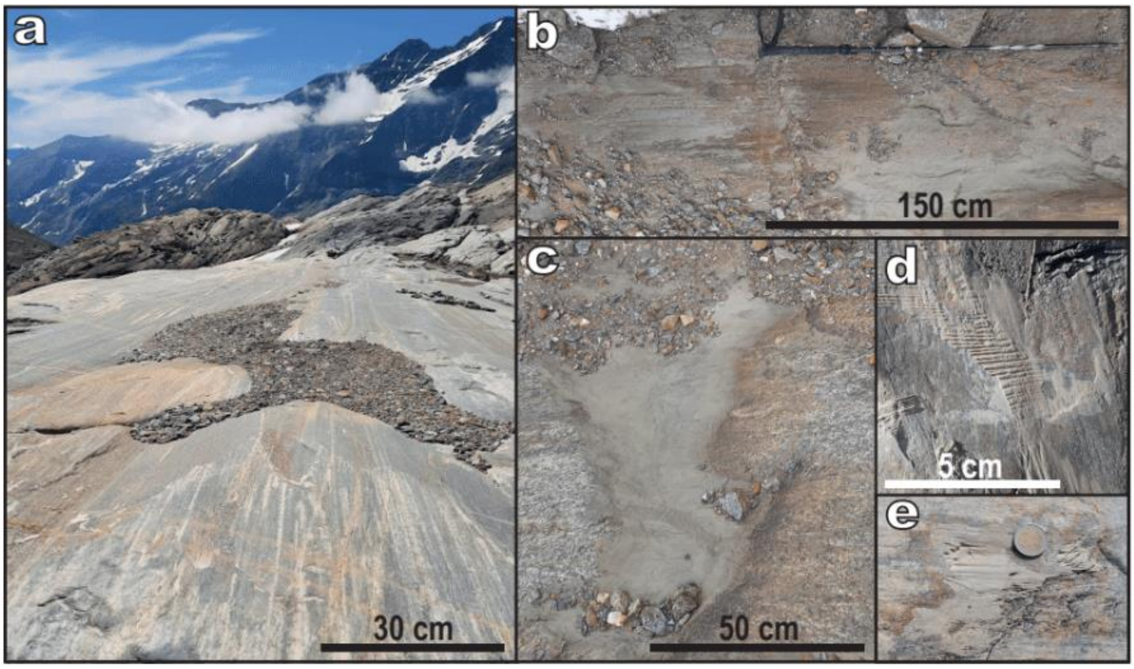

Fig. 1: Glacially striated surfaces at Wasserfallwinkel (a), and different mud layers (b-e) (© Daniel Le Heron)

Fig. 2: Millimeter thick mud layer found at higher elevations

The Großglockner and its surrounding area is part of the "Hohe Tauern National Park", which covers 1856 km^2 of the border area between the provinces of Salzburg, Carinthia and Tyrol. The way from "Franz Josephs Höhe" (2370m) to the "Oberwalderhütte" (2972m) is the so-called "Gamsgrubenweg". Along this path, some of the highest peaks of Austria can be seen.

Fig. 3: View from "Franz Josephs Höhe" to Pasterze (left) and the Gamsgrubenweg (red)

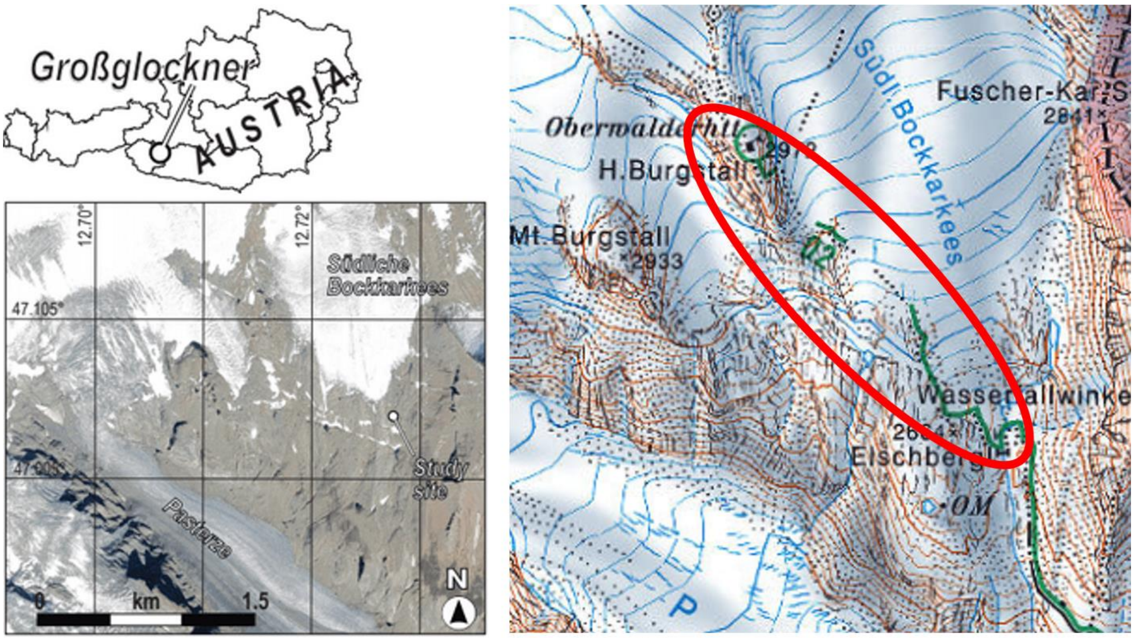

Fig.4: Left: Overview research area (© Daniel Le Heron); Right: The way marked green is called "Gamsgrubenweg", leading from "Franz Josephs Höhe" up to "Oberwalderhütte (KAGIS) *with research area in red.*

Glacial polish is a hallmark of glaciated landscapes and characteristic of rock surfaces where glaciers have passed over bedrock, typically granite or other hard igneous or metamorphic rock. It potentially holds information about subglacial conditions and processes and forms a resistant surface, that protects landscapes against postglacial weathering

(Siman-Tov et al., 2017) .The presence of such polish might be assumed to indicate exposure of the surface following glacial retreat took place relatively recently or was subsequently protected by deposition, as in the long term, this polish is expected to disappear in response weathering. In the study area, the glacial striations testify for the existence of a tributary glacier, that fed the Pasterze and covered the area of "Gamsgrubenweg".

Fig. 5: The carbonate coating layer, the lineation of the carbonate layer has the same orientation as the glacial polish below it. Position: N47°05.9552´, E012°43.4255´

Today, about 3600 km² of the European Alps are glaciated, constituting ca. 2% of their total area (Stüwe & Homberger, 2015).The largest continous sheet of ice is the region of Aletsch-Jungfrau, covering about 350 km². The largest glacier of the Eastern Alps is the Pasterze (20 km²), followed by Gepatschferner (18 km²) and Mittelbergferner (12 km²) as second and third, the latter two are both situated in the Ötztaler Alpen (Stüwe & Homberger, 2015). However, these values seem somewhat outdated as a couple of very recent data offer values of about 3000 km² - or even slightly less - for the total glaciated area of the alps and furthermore some 17 km² for the Pasterze. Accurate reconstruction of ice extent in the Quaternary is partly dependent on the recognition of classic geomorphological landforms, such as striated surfaces and other bedrock phenomena.

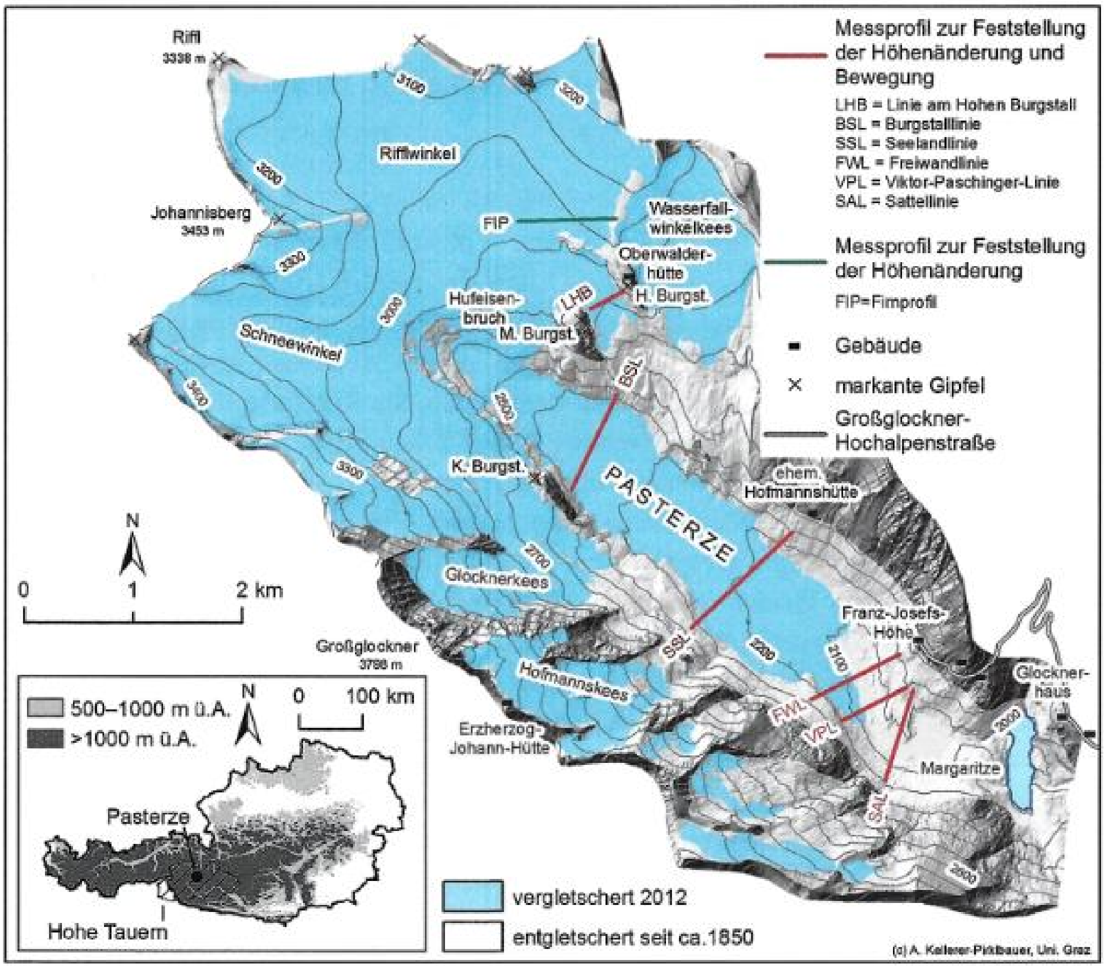

Fig. 6a: Retreat of Pasterze since the last maximum (Lieb & Kellerer-Pirklbauer, 2018, p. 32)

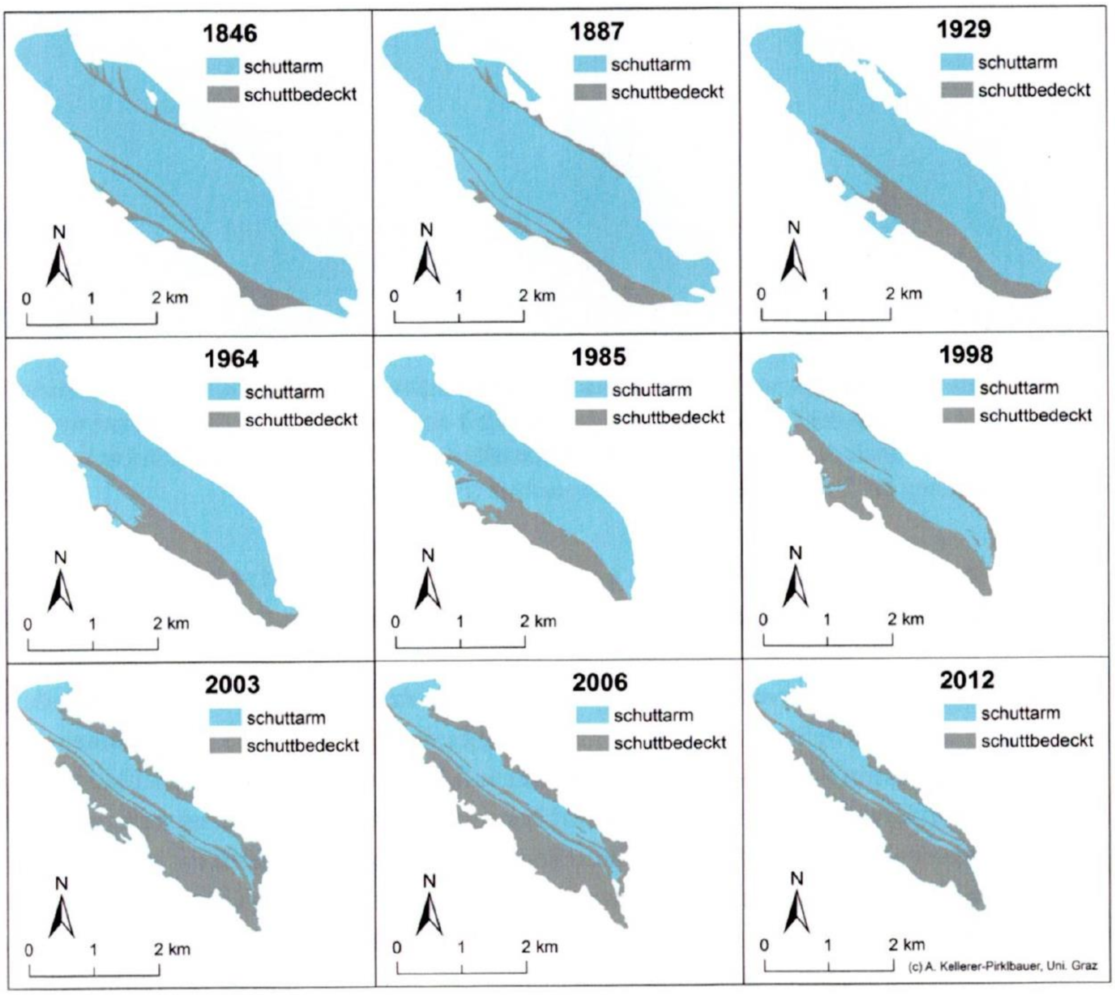

Fig. 6b: Extention of Pasterze during the last centuries (Lieb & Kellerer-Pirklbauer, 2018, p. 45)

1.1 Overview of glaciation in the Großglockner area

In 1850, the modern day Südlichen Bockkarkees glacier was subsumed into the lager configuration of the Pasterze glacier. The so-called Gamsgrubenweg - the main access point to the Südlichen Bockkarkees - was not free from ice until the mid- to late 20th century, by which time glacial recession differentiated it from the larger, Pasterze trunk glacier.

Core samples document lots of information about the climatic conditions of the last 17 000 years. It is obvious, that after the climax of the last ice age - the "Würm" period - about 20 000 years ago, there was a fast and intensive warming period in the alps, that induced the growing of higher plants, trees like arolla pine (*pinus cembra,* "Zirbelkiefer") were evidenced at places of 2150 m altitude (Krainer, 2015).

There is much more proof about warmer periods during the last 9000 years, especially in the time interval from 6000 B.C to 1000 B.C. The longest period of high temperatures, the so-called “Atlantikum”, lasted from 6000 to 3000 years B.C., with average temperatures of about 2-3 degrees centigrade higher than today (Behringer, 2011).

This period stands for the Neolithic Revolution and the era of the first high cultures. The collapse of the Indus cultures (Harappa and Mohenjo-Daro), (Kenoyer, 1991) as well as the end of the Old Kingdom in Egypt in 2150 B.C. (Wilson, 1961) and of the Akkadian Empire in Mesopotamia at about 2200 (Soden, 1961) might be a consequence of the climates worsening before 2000 B.C. (Behringer, 2011, p. 0). Another cold period occurred around or shortly after 1200 BC. (Falkenstein, 2012/13). The latter coincides with historical events like the Dorian Migration and the invasion of the Sea People into the Mediterranean Area (Wilson, 1961).

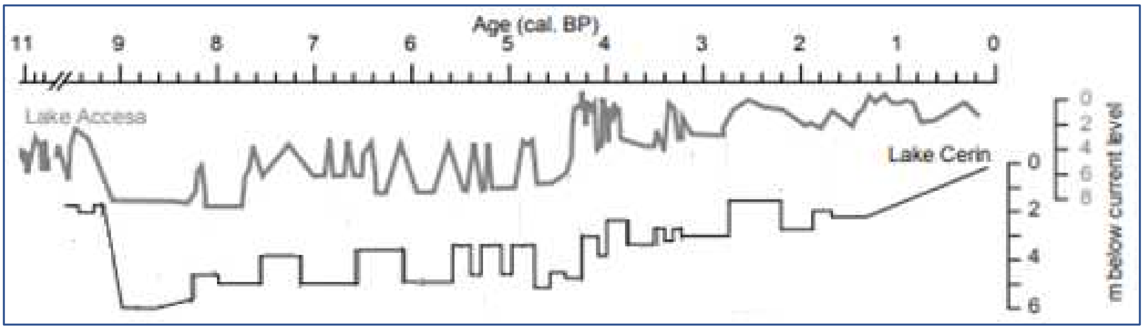

Fig. 7: History of hydrological conditions of two lakes (Lake Cerin in central France, Lake Accesa in central Italy), showing a pronounced climatic change starting at 2300 B.C (4300 years from now) (Arnaus et al., 2012, p. 92).

An additional warm time interval – the so-called “Roman warm period” – lasted from about 300 B.C until 400 A.D. and was followed by a much colder era from 400 to 700 A.D., where the glaciers had reached extensions similar those of modern times. Thereafter, the medieval warm period followed, with average temperatures of about 1 - 1.5 °C higher than today. Around 1250, a slow decrease in the temperature was initiated, which became more and more pronounced. The Viking settlers in Greenland suffered from that process and died from starvation around 1500 (Ross-Macdonald, 1971, p. 209) and (Wernick, 1980, pp. 153-154). That trend finally culminated in the so-called “Little Ice Age” (LIA) from 1600 to 1850, with average temperatures about 1 °C lower than those of the present days. The LIA is associated with 3 ice maxima phases, namely in 1620, after 1700 and 1850.

The latter maximum produced large latero-frontal moraines that are found at many modern glacier margins (e.g. at the Gepatschferner; Le Heron et al., 2022) but destroyed the earlier medieval moraines (Krainer, 2015).

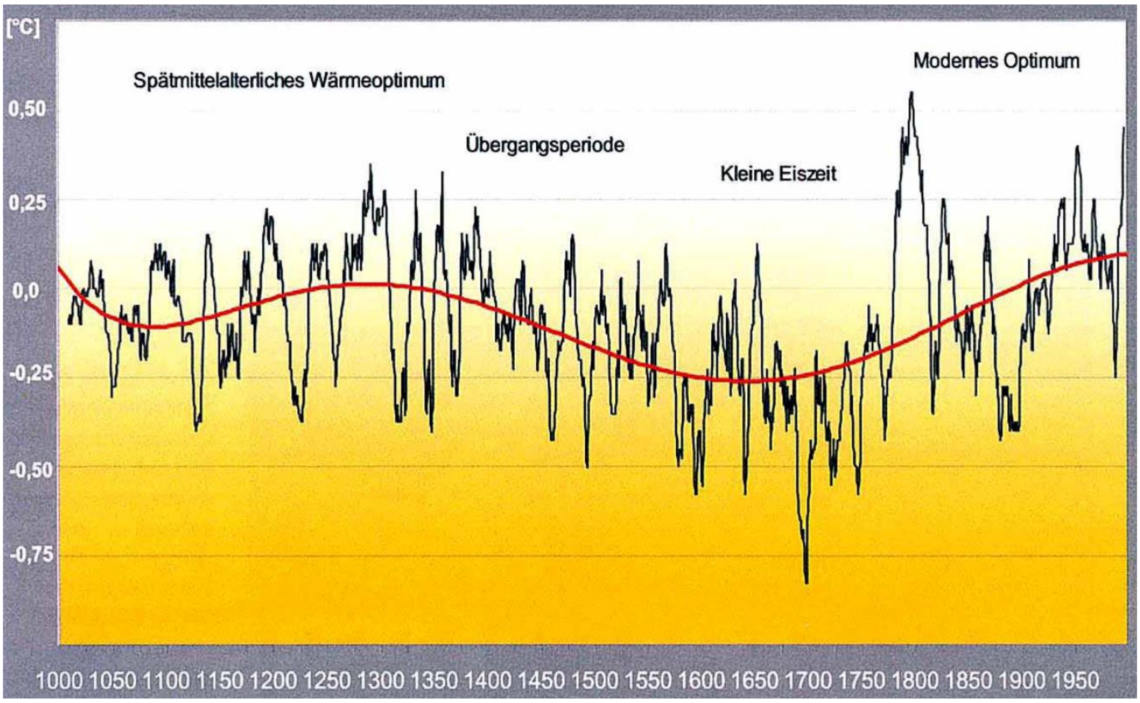

Fig.8: Short-term and long-term variations of temperature during the last 1000 years in central Europe (Behringer, 2011, p. 104)

In general, shorter-term fluctuations of ice volume need not to be directly coupled with climatic variations, rather driven by internal processes within the glacier system. The Pasterze, specifically, ia known as a quite inert glacier which tends to mirror only long-term variations of temperature:

„Gletscher sind eine der wesentlichsten Quellen für die Erfassung der Klimageschichte, da sie (…) gerade längerfristige Änderungen sehr empfindsam durch Größenänderungen widerspiegeln. Die Pasterze gehört zu den "trägen" Alpengletschern, was sich aus der vergleichsweise großen Anpassungszeit (…) von mindestens 30 Jahren ablesen lässt." [1] (Nicolussi, 2011, p. 24).

Whilst glacial geomorphological features may testify to larger ice volume during the LPIA, perhaps more remarkable is the occurrence of fossil wood material found both in front of the modern glacier environment and, in some cases, encased within it (Nicolussi, 2011).

[1] My own omissions.

Such evidence for warm intervals during the early and mid-holocene came from samples of wood and peat, found both in the outwash plain in front of the glacier tongue and within the present day glacier. Radiocarbon dating indicated different ages, up to 9000 years (Krainer, 2015). These results correspond to annual growth ring data reported by Nicolussi. No plant samples were found in situ, that is on their original place of growth. The material had been preserved below the ice for some thousands of years in the area of the recent glacier tongue before it was washed out from there. That attests to a period of growth on ice-free locations even on places, that yet are still covered by the glacier. Each of the ice-free periods seem to last at least a couple of hundred years, but they were separated from each other from time to time by a new glacial advance (Nicolussi, 2011).

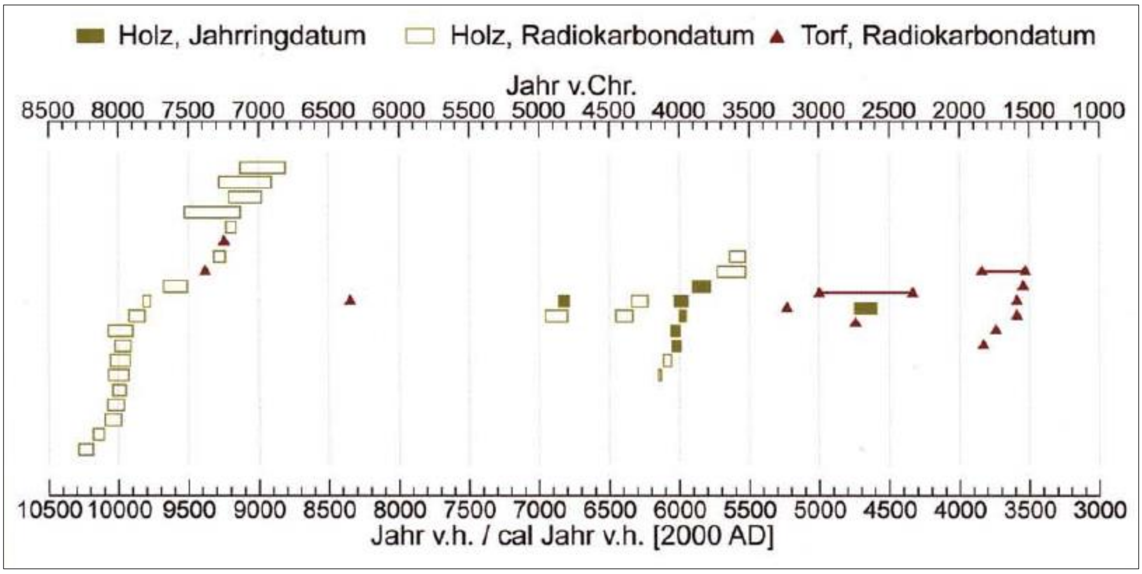

Fig. 9: The chronological allocation of samples of wood and peat from the front of the Pasterze, in accordance with datings from annual rings and radiocarbon-dating. (Nicolussi, 2011, p. 26).

1.2 Classification of glaciers

Glaciers may be categorized by different criteria by their dynamics, their morphology or by thermal conditions. The thermal classification is in this context the most substantial one. The principal criterion here is the temperature of pressure melting. That means the reduction of the temperature of ice-melting, caused by the glaciers self-weight at its base. The static pressure of 100m ice reduces the melting point at the ground by approx. 0,06°C. But the temperature of ice and water is influenced by a couple of factors besides ambient temperature, namely irradiation and exchange of air mass, further by soakage, by infiltration of crevasses with water from rain and by geothermic flow (Schrenner, 2011).

Schrenner (2011) continued with the description of the three principal types of glaciers, basing on their thermal status, which briefly are:

1) Temperate glaciers – also called warm-based glaciers – located in the middle or low latitudes. The temperature of their ice is close to the pressure melting point. Therefore, they produce melting water during the whole year, which results in a continuous film of water on the glaciers base. Irregularities of the ground may lead to fluctuations of pressure and temperature. A possible consequence can be regelation, i.e. melting and recrystallization of the ice. The process of regelation causes an alteration of form and crystal texture of the ice, which, together with the temperature at the pressure melting point, contributes to the soft plasticity of tempered glaciers and their plastic flowage. Temperate glaciers react to alteration of climate with advance or melting.

2) Cold glaciers are mainly found in the polar regions of earth. These are characterized by the total absence of liquid water, i.e. no film of water underneath, and thus the ice is frozen to the ground. The ice deforms in a brittle manner in case of a movement of the glacier.

3) Polythermal glaciers share common elements of the preceding examples. Temperatures near the pressure melting point are located in the glaciers accumulation zone, whereas the temperatures in the ablation area are typical for cold glaciers. (Schrenner, 2011).

It is obvious from this classification, that Pasterze is an example of a temperate glacier. Additional confirmation is obtained from the fact, that a small brook, called “Möll”, that has its source from the Pasterze, is water-bearing both in summer and in winter (Kirchlechner, 2011). One may assume, that the coating layer, that I had found, is a result of the glaciers movement and might therefore most probably be restricted to the ablation area of temperate glaciers.

1.3 Coating layers on glacial surfaces: a brief introduction and review

Glacially striated surfaces are commonly regarded as purely erosional phenomena, and typically evidence a combination of abrasion processes (striations, grooves of different geometries) together with a host of meltwater-generated phenomena called p-forms (Kor, Shaw, & Sharpe, 1991). The suite of erosive structures are classic and include a variety of dm- to m-scale meltwater structures that can be recorded from pristine Ediacaran surfaces (Le Heron et al., 2019) as well as in Alpine environments (Le Heron et al., 2022). Cryogenic deposits, comprising mm-scale laminations coating striated bedrock surfaces, are widely reported but poorly understood. This is despite the fact that such deposits have much to reveal in terms of meltwater processes at the ice-margin interface. Globally, previous work has identified two principal types, namely (i) silica-rich coating layers and (ii) carbonate-rich coating layers. Here, these two types are briefly introduced and reviewed.

1.3.1 Silica-rich coating layers

Siman-Tov et al. (2017) undertook investigations in the Yosemite National Park where they described a coating layer situated on the glacial polish of a granitic substrate. The following serves as a summary of their findings. The researchers found layers of amorphous material having a thickness ranging from µm to mm scale. Thin sections, SEM investigations and elemental analyses together revealed a material composed of some thin layers of different composition, some amorphous, some phyllosilicate, and all derived from granodiorite bedrock. Obviously, the glacier scraped material from the rocks and ground it into a thin paste like layer to produce a very thin mineral veneer across the rock surface. The impermeable nature of this surface inhibits colonization by lower plants and thereby slows chemical weathering. Therefore, it may protect the glacially polished surface and conserve it for long periods (Siman-Tov et al., 2017).

1.3.2 Carbonate-rich coating layers derived from carbonate bedrock

Whilst the descriptions above by Siman-Tov et al. (2017) may apply to broadly siliceous or granodioritic substrates, they do not apply directly to the Wasserfallwinkelkees area, where a carbonate veneer is recorded. My material seems somewhat of more thickness, but less hard. Other precipitates at the sole of temperate glaciers were already found in the Rocky Mountains as early as 1970, and they were described as similar to travertine (a porous rock consisting of calcium carbonate) (Ford, Fuller, & Drake, 1970). Hallet did describe such patchy carbonate coatings from the Rocky Mountains and interpreted these to have formed as result of chemically precipitation under moving ice. In this model, $CaCO_3$ is dissolved from the bedrock at the stoss side of obstacles and was thereafter deposed on the lee sides by regelation processes (Hallet, 1976).

In Europe, similar glacial deposits of carbonate have been found in the remnants of the Triglav Glacier, located in the Julian Alps in Slovenia. This is a kettle glacier (also called glacieret), meaning an icefield of a few hectares in size, nourished mainly by snowfall or avalanches, without accumulation area and glacier tongue (Tintor, 1993). The thin carbonate deposits found there – they will be eroded in a matter of decades – consists of mixture of calcite with small aragonite inclusions. Dating by the uranium-thorium method gave a series of ages: 23 600 y, 18 500 y, 12 700 y, and in a different set of samples 3 850 y and 1 960 y. Radiocarbon dating for organic matter (charcoal and wood) found in a terminal moraine 300 m below the present ice patch gave an age of about 5 500 y (Lipar et al., 2021).

The Glacier de Transfleuron, on the east of Les Diablerets in the Bernese Alps, provides another example of carbonate deposits, where three different types of calcite precipitate are recorded. Two of them, sparite and micrite, may easily be explained by progressive freezing of the subglacial water film. However, the third one, a white deposit, that had unusually heavy $\delta C13$ values, is less understood Sharp et al (1990). Such $\delta C13$ It could be interpreted as the result of calcite precipitation in equilibrium with atmospheric CO_2 or alternatively as a result of fractionation due to photosynthetic removal of C12 from the substrate by cyanobacteria (Sharp et al., 1990). During photosynthesis, cyanobacteria and plants prefer the lighter C12, an alteration in the isotope ratio is therefore an indication of biological activity (Treydte et al., 2004).

1.3.3 Carbonate-rich coating layers derived from non-carbonate bedrock

The preceding example refer to locations where glaciers have eroded limestone bedrock substrates. Nevertheless, there are several published examples where carbonate-rich coating layers are found on non-carbonate substrates, and where constituent Ca-bearing minerals play an important role. Some of these deposits occur beneath cold-based glaciers, some beneath polythermal glaciers, and others beneath temperate glaciers. One such example is the so-called Glacier No.1.

In the Tianshan mountains, of Xinjang, there is a glacier, that in principle belongs to the cold glacier category, however whose base approaches the melting point and shares characteristics of a temperate glacier in part (Liu et al., 2005). Here, the bedrock comprises augen gneiss, diorite and quartzitic shist; the coating layer is dominated by calcite (>90%), with accessory illite, chlorite and quartz. The shape of the deposits reflects the shape of solid rock underneath. Rhythmic lamination of light-coloured crystal laminaes alternating with dark-coloured detrital layers occur on the micron scale. This rhythmical layering of the deposits was posited to result from periodic changes of the thickness of 1-100 µm thick, subglacial water film. The water film that deposits these layers is considered to be ephemeral (Hallet, 1979). It remains unclear if that is the result of annual fluctuations or derives from variations on a different timescale.

2. Further Introductory Information

2.1 Chemistry of carbonate coating layers

Carbonate coating layers on crystalline bedrock appear to be widespread and are reported from the Antarctic (Aharon, 1988), on central Baffin Island (Refsnider et al., 2017) and from Scandinavia (Samuelsson, 1964) (Kers , 1964). In some cases, the origins of Ca and C in these places are poorly understood, but a contribution from atmospheric CO_2 (Kers, 1964) is speculated, whereas on others, the source of Ca is linked to weathering of Ca-bearing mineral phases and C from organic (plant) debris entrained by the glacier (Refsnider et al., 2017). The group examined palynomorphs (pollen, spores, etc.) and hypothesized that these were derived from thin Tertiary sedimentary strata that were removed from their origin by ice-sheet erosion during Pleistocene (Refsnider et al., 2017).

At Glacier No.1, the production of carbonate coating layers is explained by the following reaction (Liu et al., 2005):

$$CaAl_2Si_2O_8 + 2H^+ + 2OH^- \rightarrow Al_2Si_2O_6(OH)_2 + Ca(OH)_2$$

$$Ca(OH)_2 + 2CO_2 \rightarrow Ca^{++} + 2HCO_3^-$$

whereby bicarbonate, derived from CO_2 in the snow and ice, will take part in this process, forming the hydrogen carbonate of calcium, which is in chemical equilibrium with carbonate, depending on the pH of the solution. In the case of Glacier No. 1, the deposits had lower content rates of K, Na, Si, compared to the content rate of Fe, which is an indication of some alkalinity, that will favor carbonate against bicarbonate in the equilibrium (Liu, et al., 2005). (Iron compounds are less soluble in alkaline solution and they will therefore accumulate in the precipitate, whereas the solubility of alkali metal compounds is high and unaffected by the pH). Although the initial concentration of calcium carbonate is probably much too low for the precipitation of carbonate, the process of regelation may result in a high increase of the carbonate concentration in the remaining liquid phase and therefore in its sedimentation.

As the bedrock described above does not contain any limestone, the deposits could not originate directly from there. The source of these carbonates therefore might be different from those found under the temperate glaciers in a limestone area like the Rocky Mountains and the South-Alps, where the layers may come from products of decomposition of calcium carbonate minerals in the subglacial bedrock (Liu et al., 2005). However, as all these structures are quite similar in limestone and not-limestone areas, the question is opened, if not all are formed by the same precipitation process that has very little to do with the bedrock categories or the glacial types (Liu et al., 2005).

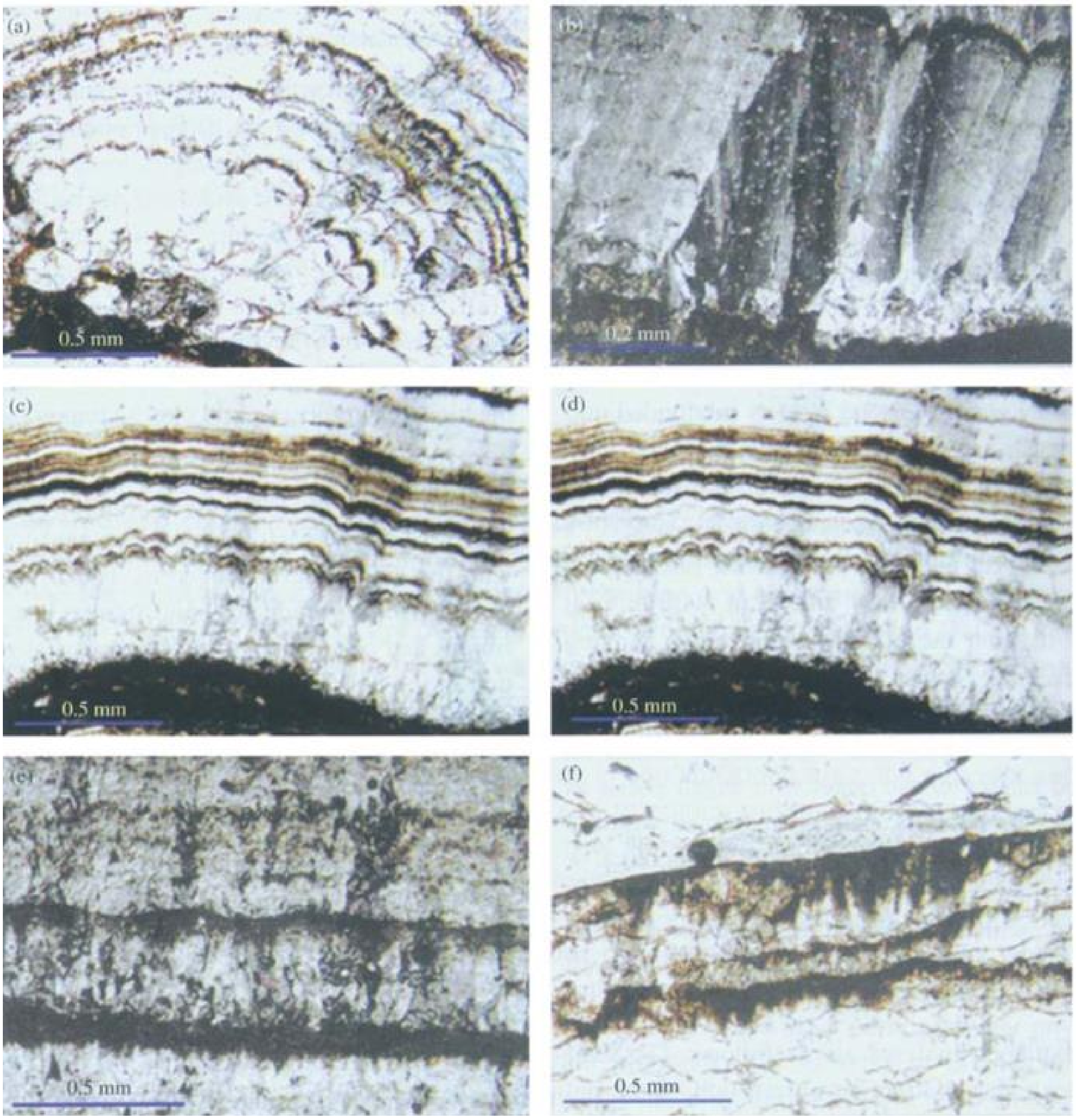

Fig.10: Sedimentary structures found by (Liu et al., 2005, p. 1472); Note the similarity with my own samples described below

2.2 Carbonates precipitated beneath temperate glaciers

For a temperate glacier, similar data have been described by a group of french scientists for the Bossons glacier in the Mont Blanc Massif. They were first to describe SPSSs (subglacially precipitated carbonate crusts) on a bedrock of plagioclase and amphibole in Europe. These crusts had been formed on the lee sides of “roche moutonnée” (also called “sheepback, a rock-formation created by a passing glacier (Carol, 1947) and were very recently exposed by the retreat of the glacier. The French investigators disbelieve the most common model assuming that the SPCCs form out of $CaCO_3$ from the bedrock when meltwater becomes supersaturated on the lee side of an obstacle during the regelation process. Some locations are described where SPCCs have been found in the absence of sedimentary carbonate sources (Thomazo et al., 2017).

At the Bosson glacier, carbonate crusts are 5-10 mm thick. The samples were arranged in tiers of numerous laminae, each of a few micrometers, with alternating light- and dark-colored bands. The mean δC13 value of the SPCCs is -11.3 ± 0.5 ±‰. Microbial respiration might be responsible for such light δC13 record for carbonates, however neither epifluorescence and CLS Microscopy, nor Raman spectroscopy support the presence of an active microbial community. Moreover, the carbon could originate from the combination of abiotic and biotic oxidation of organic material trapped in the subglacial preserved soil (Thomazo et al., 2017).

The source of calcium is obviously the calcium silicate minerals from the granite-gneissic basements. On the other hand, the main source of carbon is the soil organic carbon that came from organic remains, i.e. from vegetation growing at high altitudes during the Holocene climate optimum. (Thomazo et al., 2017)

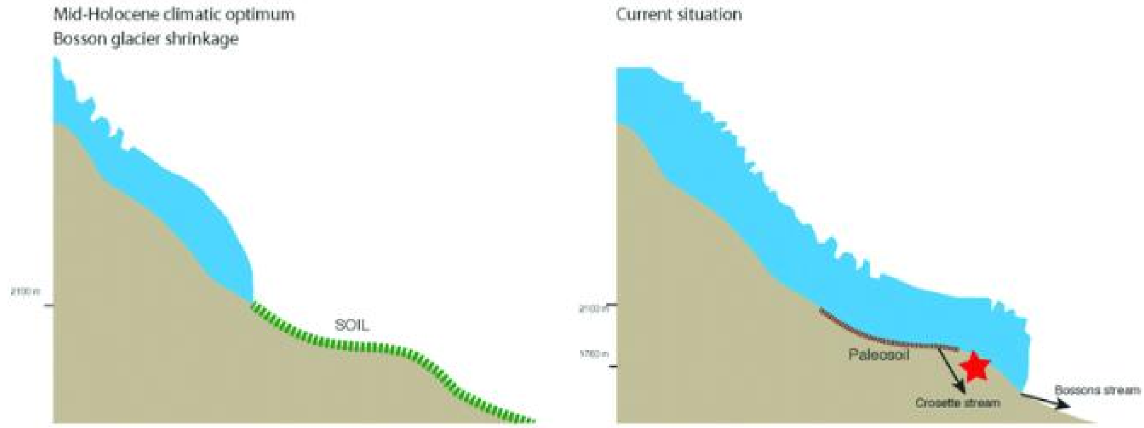

Fig.11: Simplified representation of the Bossons glacial extension during the Holocene climatic optimum (left) and at present (right). The red star represents the location of subglacial precipitated carbonate crusts retrieved during the course of this study (Thomazo et al., 2017, p. 13)

"The carbon isotopic composition of the SPCCs show, that the "dissolved inorganic" C required for the Bossons Glacier cryocarbonate precipitations is largely derived from organic material trapped in soils overridden by the glacier and oxidized in the subglacial environment" (Thomazo et al., 2017, p. 12).

The accumulation of large amounts of organic material indicates that the glacier was in a retracted position - quite more reduced than recently - for a longer period and that the cryocarbonate reflects the soil organic carbon of a minimum age of 6 500 years. This agrees with the Holocene warming period between 9 300 and 6 000 years cal BP, especially with the period III, which occurred after 7 000 years cal BP. Further do this evidence neatly correspond with the dating of the samples of wood and peat described by Nicolussi (see above, Fig.9).

2.3 About climate fluctuations during and after the last ice age

The last one of the ice ages - called Würm glacial stage in the alp region, but Weichsel glacial stage in northern Germany – lasted about 100 000 years, from about 115 00 BP until about 12 00 BP (Jürgen, 2020). But in the course of this time interval, a couple of warmer periods did occur. It is somewhat controversial in literature, the Würm period could be subdivided into two periods - ´Altwürm´ and ´Hauptwürm´ - or better in three periods - ´Altwürm´, ´Mittelwürm´ and ´Spätwürm´, but it is generally agreed that there was a distinct warming interval before 25 000 BP, separating ´Altwürm´ from the later glaciations (Gross, 1956).

Gliederung der letzten Eiszeit

In Europa: Würm-Eiszeit				In Nordamerika: Wisconsin-Eiszeit			
Haupt-abschnitte	Phasen	Kulturen	C14-Daten (v. Chr.)	Haupt-abschnitte	Phasen	Kulturen	C14-Daten (v. Chr.)
	Spätglazial	Swidérien im Osten Ahrensburg Spätmagdalénien Hochmagdalénien Hamburger Stufe II Hamburger Stufe I östl. Gravettien	8 000 8 300 9 000 12 000 13 200 14 000		Spätglazial	Folsom Bi-son-jä-ger Midland (Texas)	8 000 9 000 9 250 10 000
Haupt-Würm	Aufhören der weiträumigen Lößablagerung Jungwürm (spätes Hochglazial b. z. Pomm. Stadium einschl.)	? Frühmagdalénien Solutréen östl. Gravettien		Haupt-Wisconsin	Hoch-glazial	Llano-Kultur	
	Paudorfer Interstadial	spätes Aurignacien				(Elefanten-jäger)	19 550
	Mittelwürm (frühes Hochglazial)	spätes Aurignacien mittleres Aurignacien Präsolutréen II	22 000			Kameljäger	〉21 850 22 000
Göttweiger Interstadial (temperiert) = Spiezer oder Laufen-Schwan-kung. Dauer vielleicht ca. 15 000 Jahre		mittleres Aurignacien Präsolutréen II Spät-Moustérien	23 000	Sidney-Interstadial (temperiert) in Ohio Dauer vielleicht 16 000 Jahre		Zwerg-mammut-jäger von Santa Rosa Island (Californien)	27 700 bis 〉35 000 38 000 ?
Alt-Würm	Frühglazial	Präsolutréen I Hochmoustérien Micoquien Spät-Acheuléen	〉34 000	Alt-Wisconsin	Früh-glazial	? Sandía	
Riß-Würm-Interglazial		Micoquien Jung-Acheuléen Früh-Moustérien		Sangamon-Interglazial		1. Einwanderung d. Paläoindianer ?	

Fig. 12: Classification of the Würm ice age (Gross, 1956, p. 97)

However, the exact timing of this interval – the so called ´Göttweiger Interstadial´ - is somewhat al little controversial. Gross proposed a beginning somewhat before 34 000 B.C. and an end at about 23 000 B.C (Gross, 1956). On the other hand, Woldstedt suggested an end of this period as early as 28 000 B.C. (Woldstedt, 1958). Other authors refused the Göttweiger Interstitial and argued, that a ´Paudorf Interstadial´ between 40 000 and 30 000 BP was the dominating event. (Zötl, 1971).

Later on, Gross defined two interstadials, Denekamp (= Paudorf) at 32 000 – 28 000 BP and Hengelo at 39 000 – 37 000 BP (Groß, 1968).

Tab. 2: Gliederung der Spät- und Nacheiszeit in Mitteleuropa (nach B. FRENZEL 1967, u. a.).

Jahre vor der Gegenwart		° C ± zum gegw. Jahresmittel
3.000—4.000	Subboreal	
5.000—7.000	Atlantikum — Klimaoptimum	+ 2
8.000—9.000	Boreal	
ca. 10.000	Jüngere Tundrenzeit	— 5 ?
ca. 11.000	Alleröd Interstadial	— 3 bis — 4
ca. 12.000	Ältere Tundrenzeit	— 5 (6) ?
ca. 13.000	Bölling Interstadial	— 4 ?
ca. 14.000 bis 16.000	Älteste Dryas-Periode	— 6 ?
ca. 17.000	Lascaux — Ula — Interstadial	— 4 ?
ca. 18.000 bis 22.000	Hochglazial B (mit interstadialen Schwankungen)	— 12 ?
ca. 30.000	Paudorf — (Stillfried B) — Interstadial	0 bis — 1
ca. 40.000 bis 50.000	Hochglazial A (mit interstadialen Schwankungen)	— 11 bis — 13
ca. 53.000 bis 59.000	Brørup-Interstadial	— 2 ?
ca. 60.000	Kaltzeit	— 11 ?
ca. 64.000	Amersfoort-Interstadial	— 3 ?
	Frühglaziale Kaltzeit	— 8 ?
70.000	Riß-Würm-Interglazial	

Fig. 13: Table with temperature deviations over the last 70 000 years (Zötl, 1971, p. 197)

This controversial issue was eased by Gross, who defined a `Göttweiger Interstadial-Komplex´, that begun at 47 000 BP (or 48 000 BP) and ended around 30 000 BP. (Gross, 1960). In this concept, the Denekamp interstadial as well as the Hengelo interstadial are both minor sections of pronounced warming during a longer period of moderate temperatures.

3. Geology of the Südlichen Bockkarkees forefield and surrounding Großglockner area

The research area is located at the Tauern Window, where the rocks of the Penninic Ocean are recognizable. The limits of the Tauern Window are the Brennerpass in the West and the Katschberg-Sattel at the East (Stüwe & Homberger, 2015). The opening of the Tauern Window happened at ca. 20 Ma year ago. Inside the Tauern Window are two tectonic slices. On the one hand, the schists of the "Bündnerschiefer" correspond to former deep-sea floor (Penninic Ocean) rocks (Stüwe & Homberger, 2015) and belong to the so called "Glocknerdecke" tectonic unit. Below the Penninic-nappe in the central Tauern window, the crystalline orthogneiss of the "Zentralgneis" unit is visible. Those are parts of the Mesozoic basement, whose protolith was granite intruded at ca. 340-300 Ma. ago. (Stüwe & Homberger, 2015).

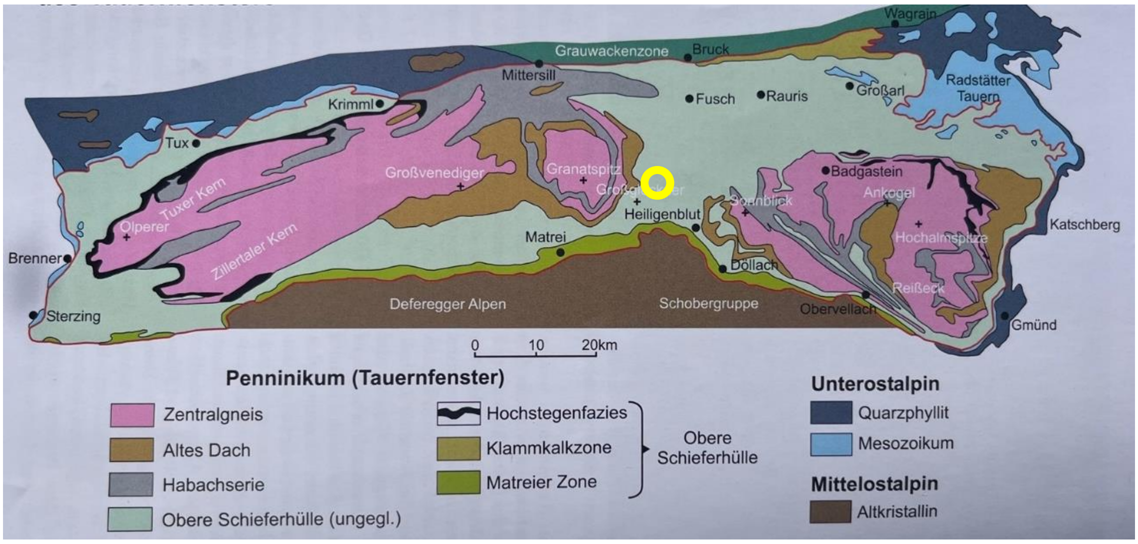

Fig. 14: Overview over the Tauern Window (according to Tollmann 1977), the research area is located at the yellow circle (Krainer, 2015, p. 28)

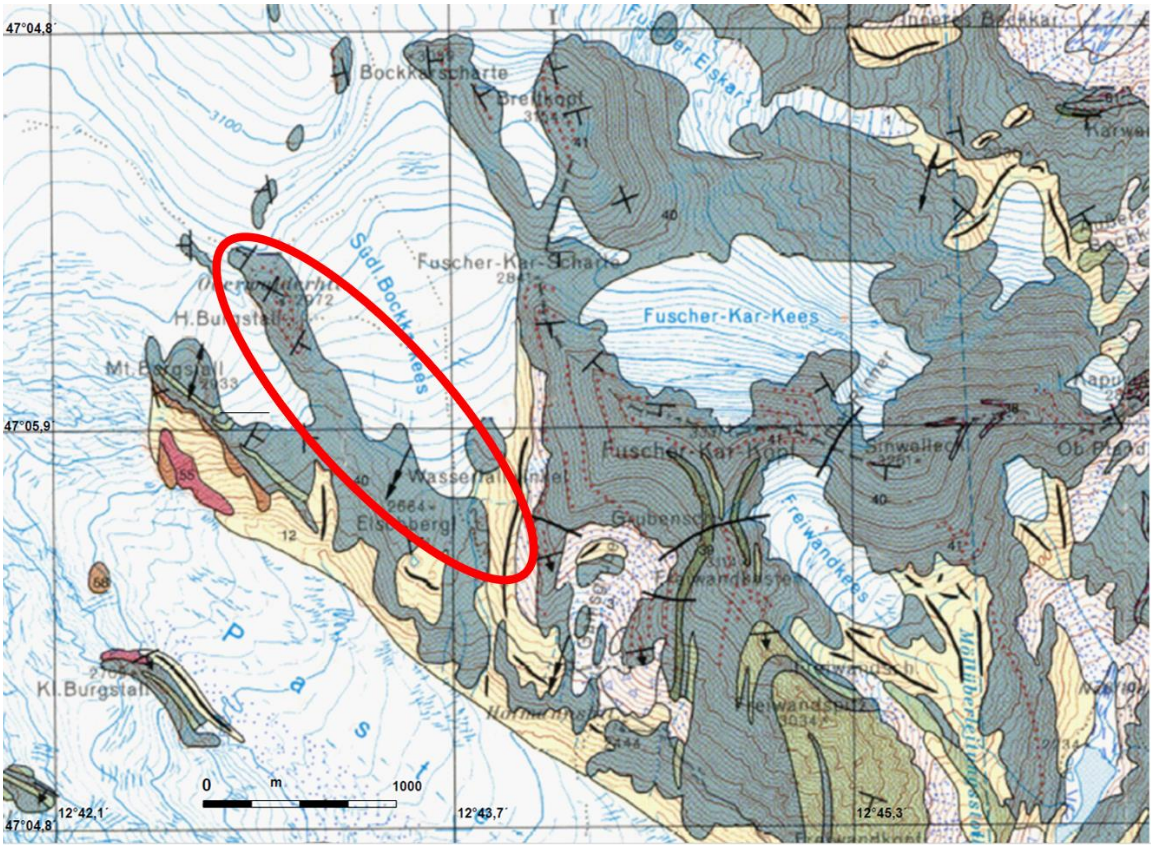

Fig. 15: Geological map of the research area, numbers 12 in yellow for the quaternary, numbers 40 in blue for the lime mica schist of the Glocknerdecke (Höck & Pestal, 1994)

The red ellipse corresponds to the area where carbonate coating layers were investigated on striated bedrock at the Südlichen Bockkarkees. The bedrock locally consists of calcareous mica schist of the Glocknerdecke, passing laterally into impure marble. These rocks are of Cretaceous age (Froitzheim, 2022). The investigated layer comes from the terminus of the Südlichen Bockkarkees (Figure 15) which formerly belong to the glacier system of Pasterze.

4. Methods

4.1 Collection of samples

The collected and later analyzed samples had been taken from areas, that recently were exposed during the glaciers retreat. The carbonate coating layers formed sports up to a length of about 1 m, distributed in the recently exposed area. Their occurrence decreases with the distance to the glacier tongue.

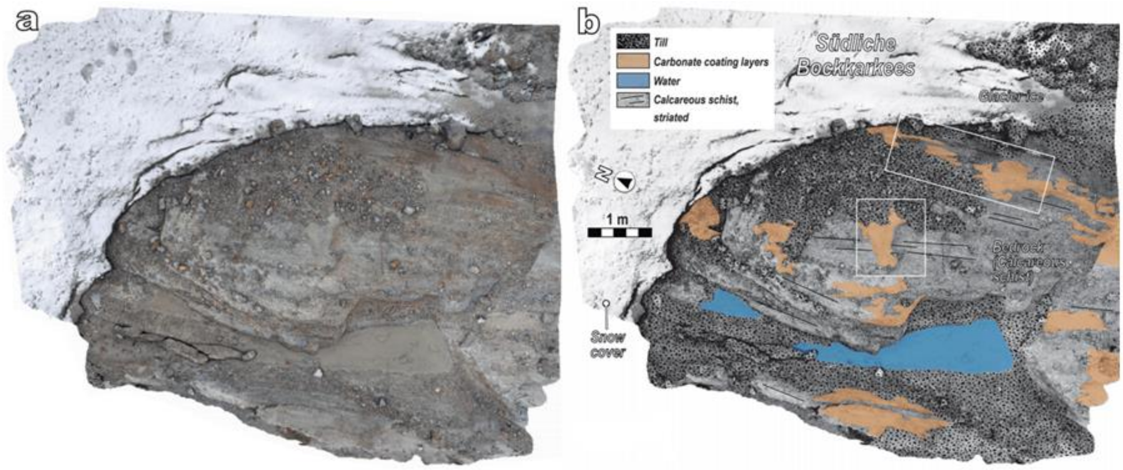

Fig. 16: Detail of an area exposed after glacier retreat (left) with the deposits and surface structures marked by colours (right) (© Daniel Le Heron).

The position of Figure 17, where this samples below had been collected is E: 12°42`33,0`` N: 47°06`27,7''. Figure 17 shows the accumulation of the carbonate layer occuring at the lee side of the bedrock's irregularities. The direction of glacial flow and glacial striation is in common with the direction of the carbonate's layers erosion. On the other hand, the inner structure of the layers, as can be seen in the Fig. 17 top left, is not in connection with the glaciers flow orientation.

Fig. 17: Sampling near Oberwalderhütte: the carbonate coatings are the light gray areas covering the darker bedrocks; the arrow marked with G indicates the direction of glacier flow

Table 1 shows the samples collected, their location and the tests carried out, which are described in more detail below.

Sample	Date / sampling	Sampling location [WGS84]	Examination of the sample
AW 1	21.09.2021	47.107694 (N) 12.709167 (E)	Thin section
AW 3	21.09.2021	47.107694 (N) 12.709167 (E)	
AW 4	21.09.2021	47.108326 (N) 12.709842 (E)	Thin section
AW 5	21.09.2021	47.108326 (N) 12.709842 (E)	XRD; C14 age / δC13 determination
AW 8	21.09.2021	47.108326 (N) 12.709842 (E)	
AW 9	21.09.2021	47.108486 (N) 12.709020 (E)	Thin section

Tab. 1: The analyzed samples with the corresponding locations

The following images (Fig.18 - Fig.20) show different manifestations of the examined carbonate layers.

Fig. 18: Sample AW3 with scale

Fig. 19: Sample AW5 with scale

Fig. 20: Sample AW8 with scale

4.2 X-Ray Powder Diffraction (XRD)

To determine the phase composition of the carbonate coating layers (CCLs), I made an analysis of one sample with X-Ray Powder Diffraction (XRD). X-Ray Powder Diffraction (XRD) is a non-destructive analytical technique, which is normally used for identification of unknown crystalline material and to determine the amount of each phase in a mixture. The sample has to be pulverized to obtain a fine powder (<10µm), which is then filled and compressed into a sample holder. This sample holder is placed in the path of the X-Ray beam, which beams at an 2θ angle from 0° to about 70°. The beam is scattered by the crystal lattice, its intensity plotted against the angle is called the diffractogram. From the 2θ angle of the peaks, the set of d-spacing's, which represent the fingerprint of the mineral, can be calculated using the Bragg´s equation (Paszkowicz, 2006).

4.3 Age determination by C14 content

The C14 content of a living organism is in equilibrium with the atmosphere, during his lifetime. From the time of death, no new C14 is incorporated, so that the C14 content decreases constantly with its half-life, that is 5730 years. This enables us to calculate back the time of death back up to 60 000 years. The primary data have to be corrected as the content of C14 of the atmosphere varied as a consequence of a change in the cosmic radiation and the Carbon cycle, the latter is influenced by the Earth's climate.

The sample AW 5 was sent by Dr. Jürgen Reitner to ETH Zürich both for radiocarbon dating and for estimation of the δC13 value. The analysis was performed by Dr. Irka Hajdas based on measurement of C14 and C13 in a sample containing carbon, carbonate and possibly some remnants of organic material. Due to the thin laminae of the sample, no separation of light and dark bands was possible, so that the results given in Table 2 are representative of the complete sequence of layers.

4.4 Determination of δC13

δC13 is an isotopic signature for the ratio of the two stable isotopes of carbon. It is defined as:

$$\delta^{13}\mathrm{C} = \left(\frac{(^{13}\mathrm{C}/^{12}\mathrm{C})_{\mathrm{sample}}}{(^{13}\mathrm{C}/^{12}\mathrm{C})_{\mathrm{standard}}} - 1 \right) \times 1000$$

The standard value is called VPDB (=Vienna Pee Dee Belemnite). A positive value indicates accretion of the heavy isotope compared to the standard.

The δC13 is dependent on the primary-production, deposit of organic carbon and the type of vegetation. During photosynthesis, a plant prefers absorbing C12 which therefore leads to a value of δC13 of about -25‰ (Treydte et al., 2004).

This evaluation was carried out accompanying with the C14 age determination described above.

4.5 Thin sections preparations and analysis

From the collection of samples, three representative samples were chosen for thin section preparation. Samples were embedded in synthetic resin, cut with a diamond saw and polished and finally mounted on a microscope slide. The thin sections were then examined under a standard polarizing microscope with specific focus on the geometry and continuity of laminae. Relationships between laminae were considered (concordant, continuous vs. discontinuous, truncations, downlaps, toplaps etc) and, as a second step, a Wheeler diagram was constructed from the observed lamina geometries (see Fig. 32. Wheeler diagram). The premise is that a thin section may reveal information about stratigraphic continuity and potentially hiatuses, using the same methodology developed for basin-scale stratigraphic analysis. This approach is piloted herein.

In 1958, Harry Wheeler introduced sophisticated chronostratigraphic charts, which are useful for clarifying the time-relationships of sediment layers (Qayyum et al., 2014). He recognized that unconformities in the layers may result from the removal of pre-existing strata, from a period of sediment bypass and from non-deposition intervals. Being a spatio-temporal plot, the usual Wheeler diagram shows in a two-dimensional chart the spatial distribution of sedimentary facies in one dimension through time in the second. This approach is now generally used as a standard procedure for describing the formation of stratigraphic relationships in time (Qayyum et al., 2017). Recently, 4D Wheeler diagrams are constructed, that use seismic data from three dimensions combined with stratigraphic thickness as a fourth dimension, but these are difficult to produce and rare. Thus, by applying this at the mm-scale, it was hoped that original insight would be possible into the deposition of the CCLs.

5. Results

5.1 XRD (X-Ray Powder Diffraction)

Table 2 shows the results of the XRD investigations. The main phase is Calcite, the minor phases are chlorite, muscovite, and quartz. Figure 21 below shows the diffractogram.

Table 2| Results of the XRD mineralogical investigations			
Sample Name	**Type**	**Main Phase (XRD)**	**Minor phase (XRD)**
AW5	cryocarbonate	Calcite	Chlorite, muscovite, quartz

Table 2: Results of the XRD analysis

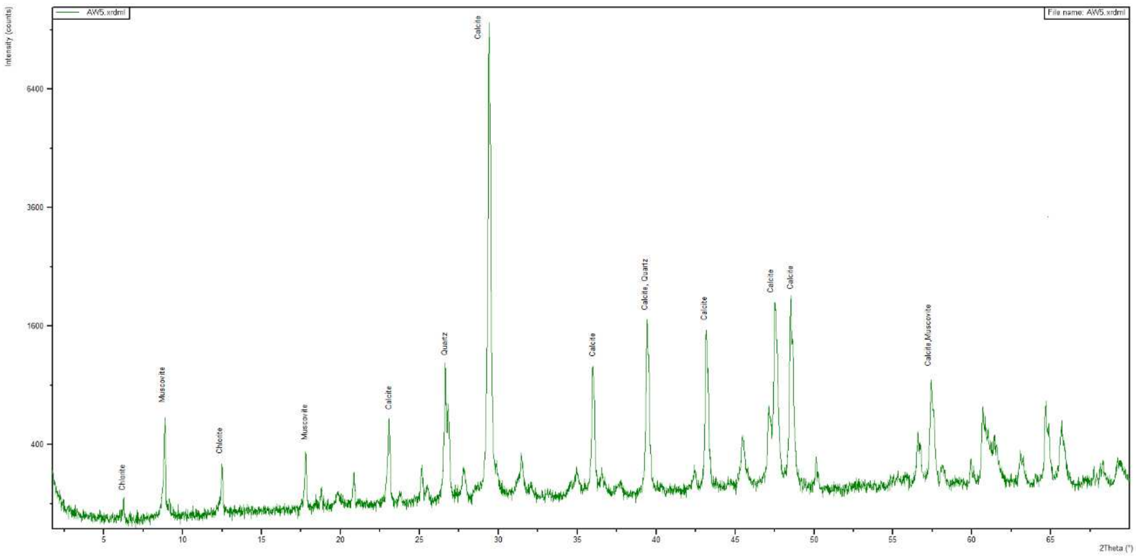

Fig. 21: Diffractogram of the XRD-Analysis

5.2 C14 age and δC13 determination

Sample	Descrip-tion*	Mate-rial	ETH	C14 age BP	±1σ	F14C	±1σ	δC13 [‰]	±1σ	mg C
AW5	subgla-cial	car-bonate	ETH-136789	38649	763	0,0080	0,0008	0,9	1,0	0,96

*carbonate precipitation; near Oberwalder Hütte from the forefield of the Wasserfallwinkelkees Glacier

Table 3: Results of the sample AW5 as obtained from ETH

The determination of sample AW5 resulted in an age of about 39 000 years, which was corrected to about 43 000 years (Fig. 22). Standard deviation of ±1σ means that the right value is located within the indicated range (±763) at a probability of 68%. The value of F14C shows in addition an age of about seven half-lives (exactly 6.95) of C14.

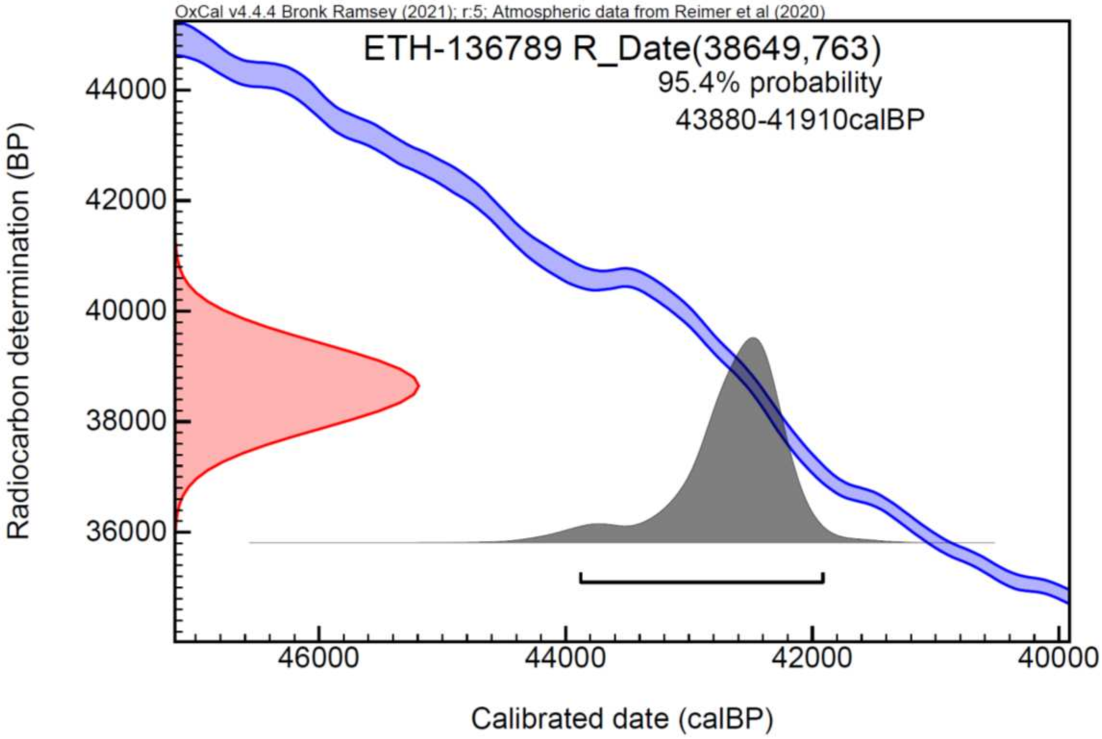

Fig. 22: C14 age of sample AW5 directly and after correction for lower C14 during Pleistocene

The result of the δC13 determination indicates a level above the atmospheric CO_2. Consequences of these data are discussed later.

5.3 Thin Sections

From a collection of samples, found at the area around Oberwalderhütte, I have selected three samples and made thin sections for further investigation.

Sample AW1 was chosen because the sample contains in situ rock below the carbonate layers.

Sample AW4 was chosen because of its unusual surface, which had formed grooves and convex shapes.

Sample AW9 was chosen because of its smooth surface, quite different compared to Sample AW 4.

Sample AW1

Fig. 23a: Sample AW1 with scale


Fig. 23b: Sample AW1 after bedding in synthetic resin

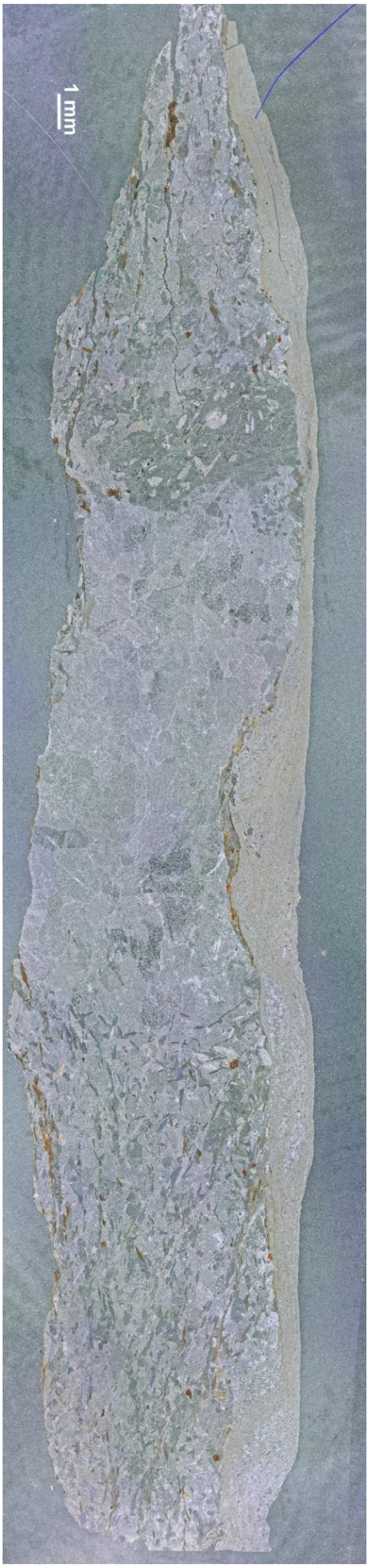

Fig.24:

Vertical thin section of sample AW1 in the microscope

Sample AW4

Fig. 25a: Sample AW4 with scale

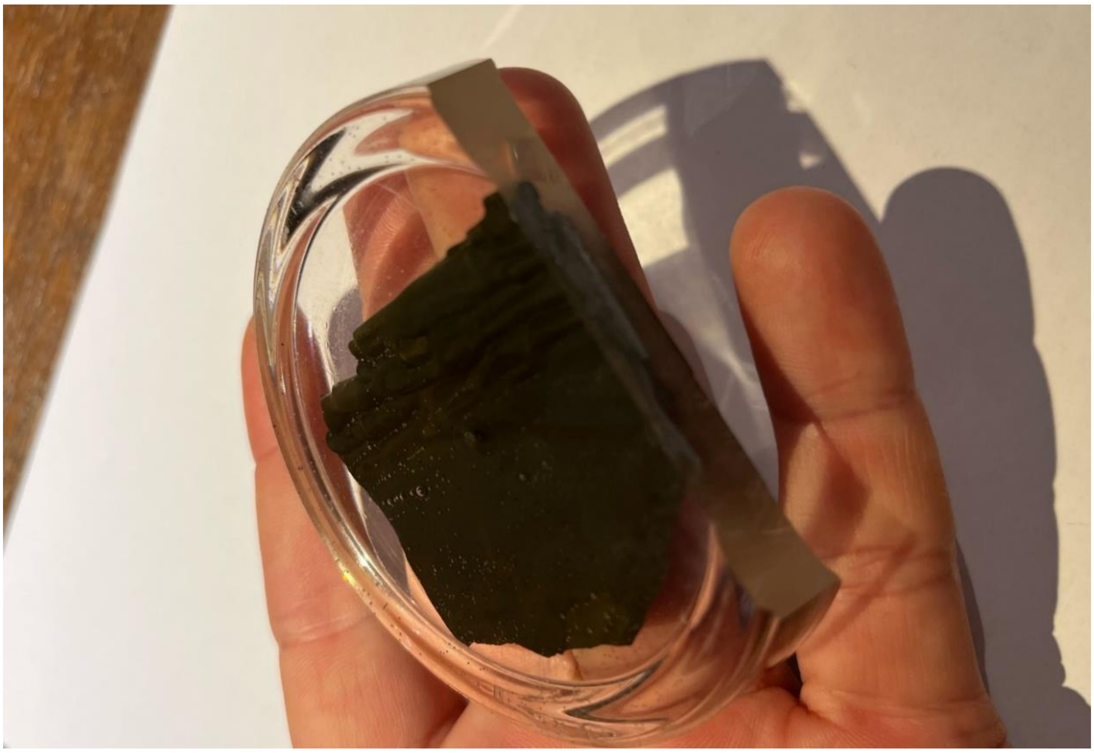
Fig. 25b: Sample AW4 after bedding in synthetic resin

Fig. 26a: *Vertical thin section of sample AW4 in the microscope*

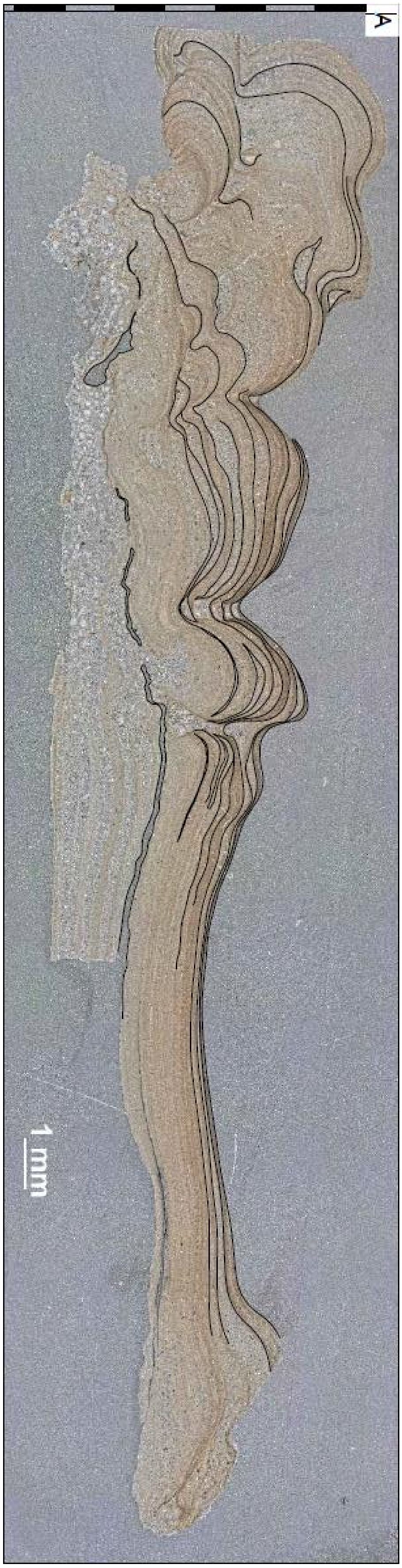

Fig. 26b: Obvious boarders from Fig.26a are plotted by Auto CAD in solid lines

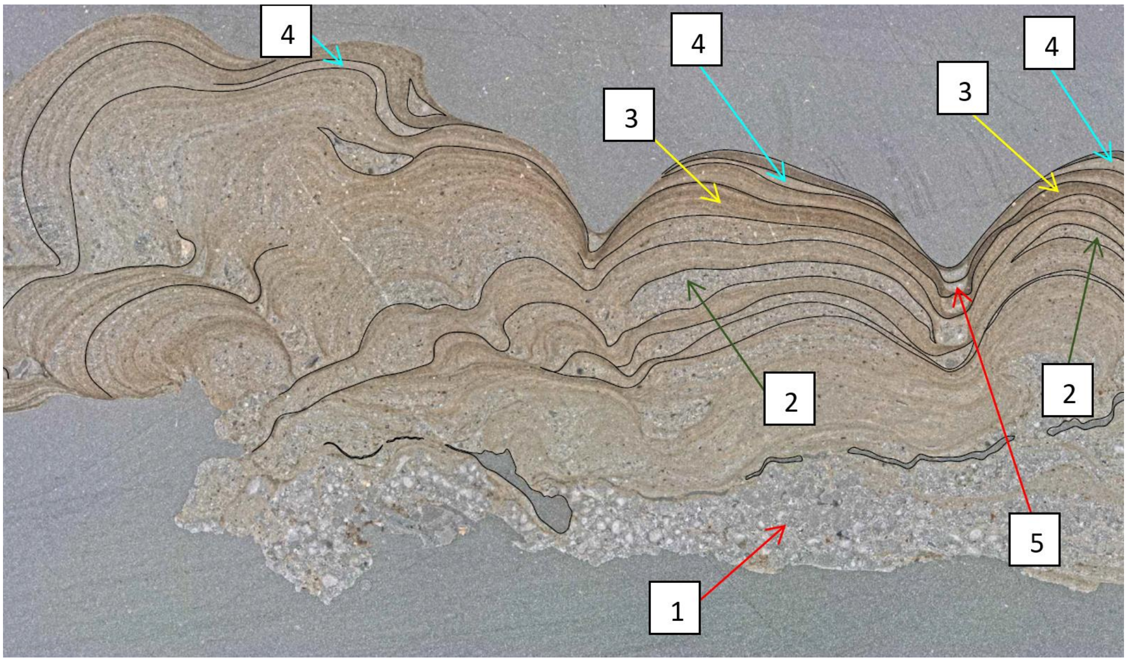

Fig. 27a: Left part of vertical thin section of sample AW4 in the microscope, the most important areas are numbered from 1 to 5

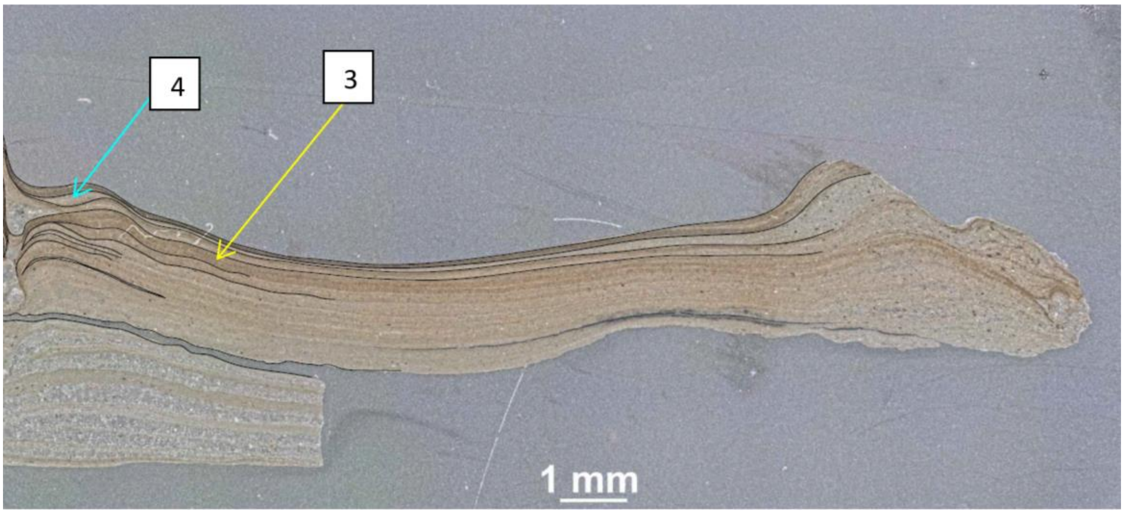

Fig. 27b: Right part of vertical thin section of sample AW4 in the microscope, showing the extension of the layers

The thin sections (Fig. 27) present the layering of sample number AW4. Position number 1 represents the solid rock below the layers. Above that there are layers, each of a different thickness, varying from half a millimeter to completely extinct. The general pattern of layers and their sequence occur in the whole thin section (numbers 2 - 4), although it is interrupted at some spots by erosion.

The position number 5 (Fig. 27) represents one of the spots, where the layers are pinched out and the space was filled up with something else, followed by the next layer. Therefore, the general pattern of layers become more complex.

Sample AW9

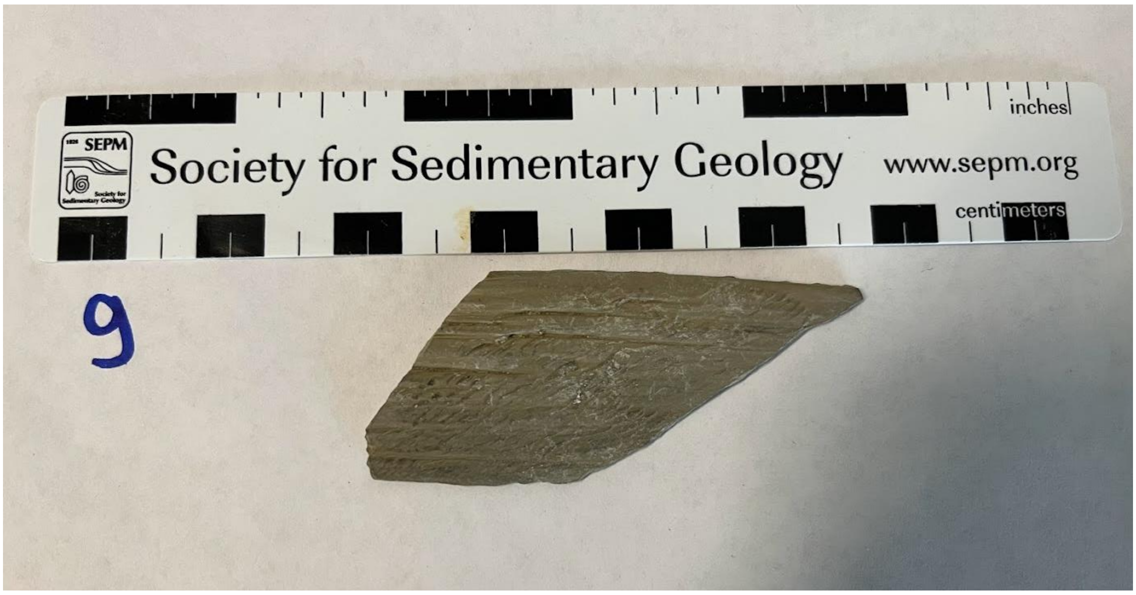

Fig. 28a: Sample AW9 with scale

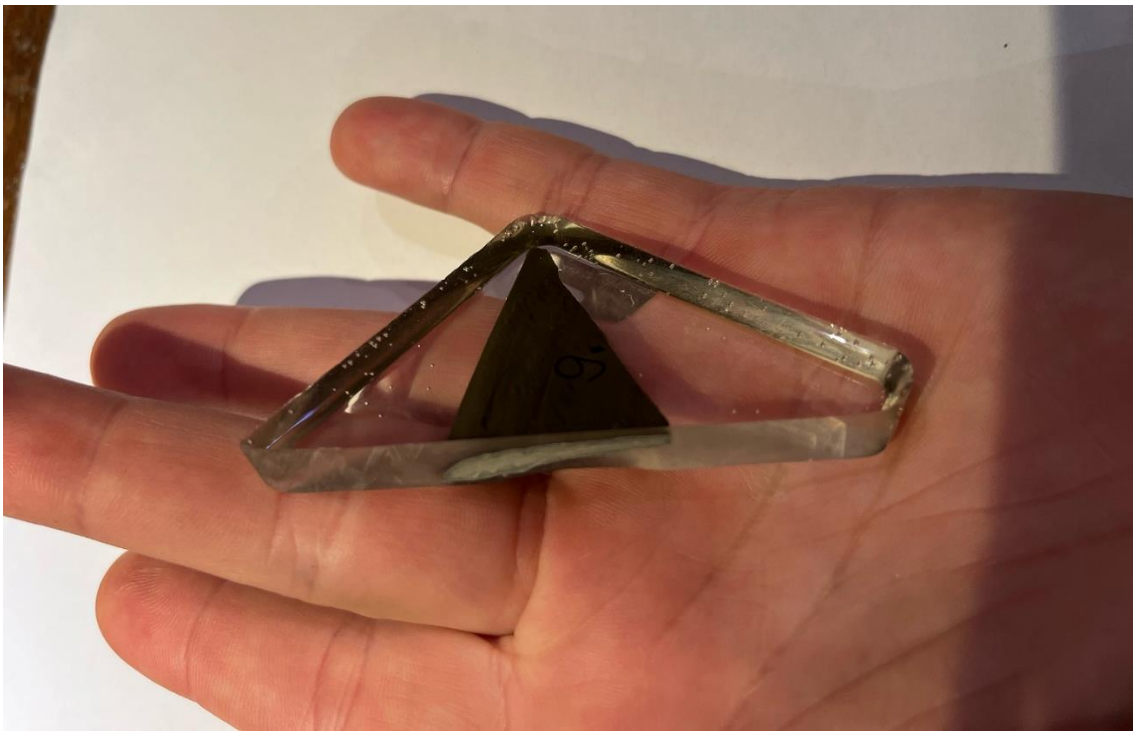

Fig. 28b: Sample AW9 after bedding in synthetic resin

Fig. 29:

Vertical thin section of sample AW9 in the microscope

5.4 Stratigraphic complexity

Thin section investigation reveals a complex stratigraphic architecture developed entirely within micrite. Micro-climbing ripple lamination, whereby stoss and lee slopes of ripples can be identified, occurs. Nested ripple trains, with discontinuous ripple geometries, can also be identified. These deposits both testify to deposition from currents, with relatively greater accommodation space (to account for laterally continuous laminae) and reduced accommodation space (to account for dis-continuous geometries) respectively. The laminations are also truncated by up to 1.5 mm deep and up to 1 mm wide micro-canyons which cut into underlying laminations and are filled with texturally identical micrite. Shallower examples, arranged side-by-side, are referred to as laterally aggrading scours. Appraising the stratigraphy as a whole, toplap and downlap geometries are recognized, together with more widely developed scour surfaces. Furthermore, there is evidence for imbricate thrusts, with sub-mm offsets and fault-bend geometries in the hanging wall, throughout the section. These geometries are particularly developed towards the top of the section. Toward the base of the section, where reverse microfaults are also present, the fault tip is sealed by overlying micrite laminae. We interpret the micro-stratigraphy of the carbonate coatings to indicate an origin primarily driven by traction current deposition, localized erosion, and intra-lamina slippage (microtectonics). The development of the stratigraphy was set against the backdrop of changing accommodation space that led to phases of erosion developing both "regionally" (at the cm-scale) and "locally" (at the mm-scale). Evidence for phases of greater sediment accommodation is provided by the more continuous laminae, together with the micro-climbing ripples which testify to high rates of sediment supply. This is because both stoss and lee slopes are preserved. By contrast, phases of reduced accommodation space are indicated by the micro-ripple lamination, with the isolated ripple crests pointing to a thinner film of water beneath the ice. Complete loss of accommodation space, at a local scale, is provided by the micro-canyons. The fact that this process occurred more widely, at least over a scale of several centimetres, is provided by the more continuous scour surfaces that traverse the section.

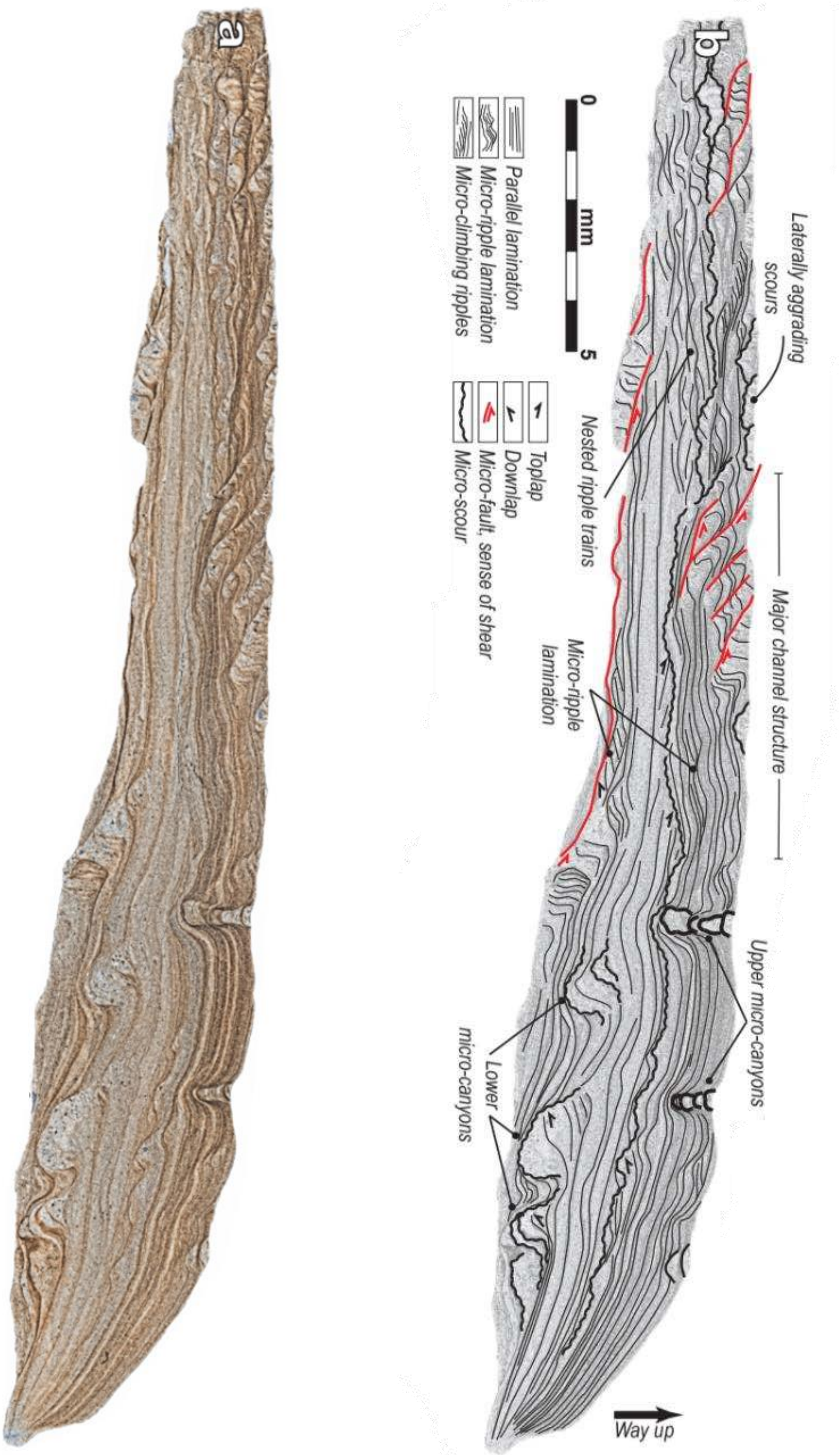

Fig. 30: Vertical thin section of sample AW9 in the microscope (left) vs. interpretation of the structure at right (©Daniel Le Heron).

Considering the structural geology, the imbricate thrusts are interpreted as the products of syn-sedimentary subglacial slippage (small scale glaciotectonic structures). Application of shear at the base of the overriding glacier during accumulation of the micrite laminae is posited to have caused slippage during sedimentation.

5.5 Wheeler diagram

Figure 31 shows the sequences of different layers, where lot of unconformities may be seen. These unconformities are a matter of later erosion processes most probably due to rising and falling water levels in different years – shown in yellow. The red lines represent some undisturbed deposits, possibly due to a total dry out during some time periods. (Note that in theory, all the yellow lines should terminate at a red line, but this is not visible in all cases.)

Below (Fig. 32), this pattern has been reconverted into a Wheeler Diagram, where the y-axis is transformed from thickness of layers into a pile of lamina representing time scale. These laminae are of equal thickness and therefore do not indicate the actual space of time, but the chronology of layers. The red and yellow bars correspond to the colors indicated above, red for undisturbed deposits, yellow for temporarily displacement of the deposits in connection with rising water level.

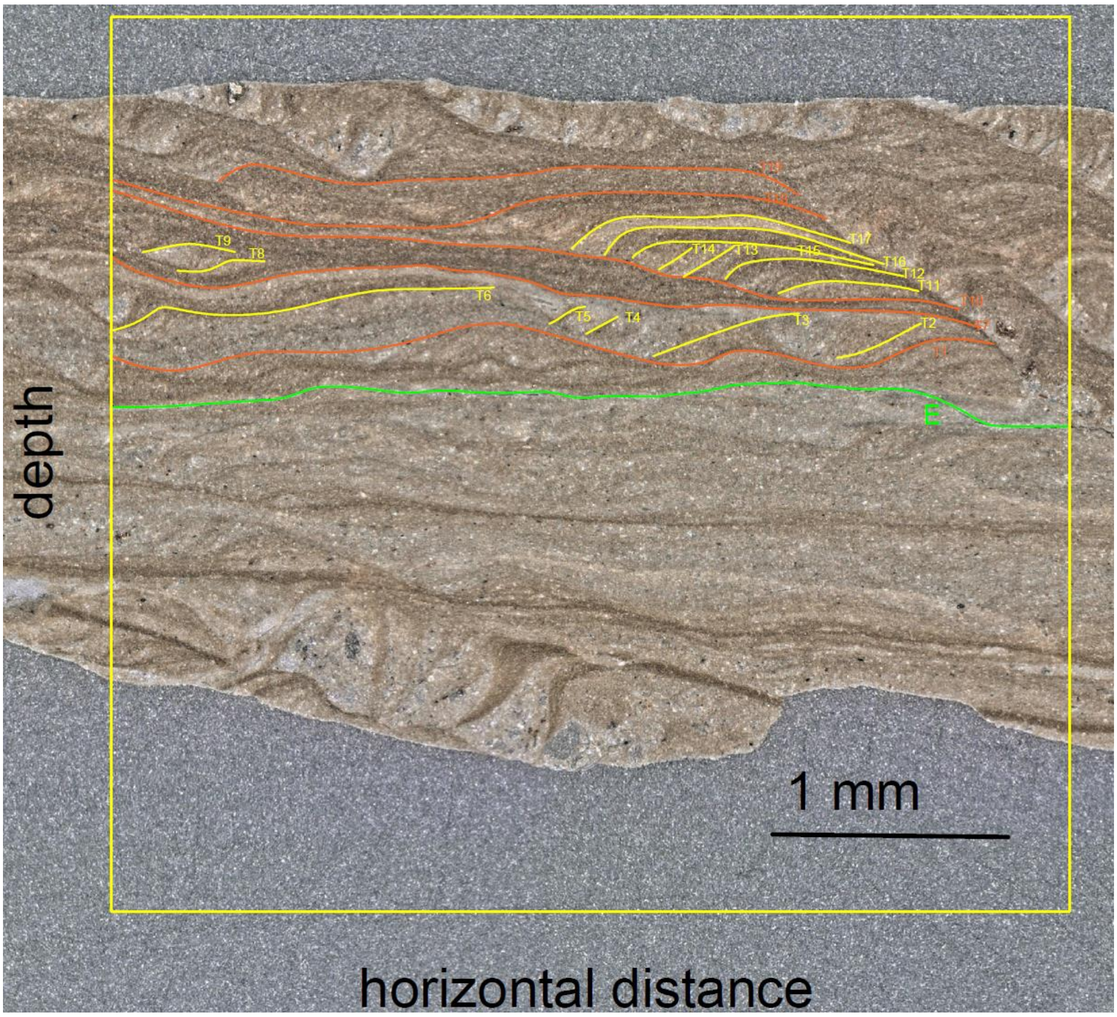

Fig. 31: Part of thin section AW 9 with different sedimentation layers from old (T1) to young (T19)

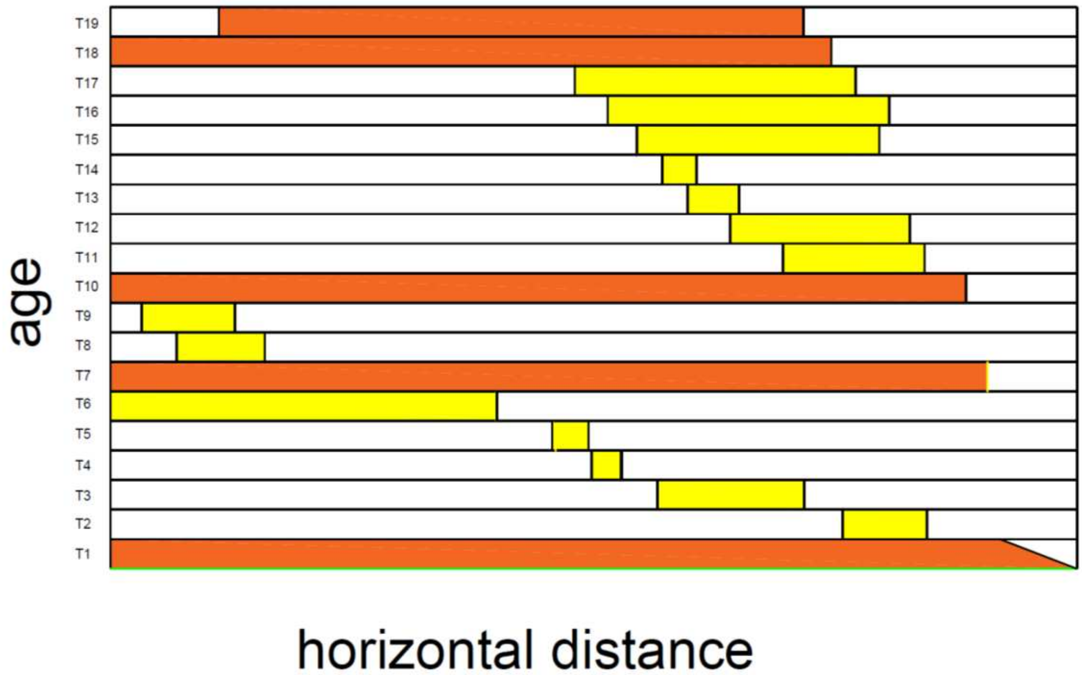

Fig. 32: Wheeler diagram using the layers from above. Red for undisturbed deposits, yellow for local deposits as a matter of changes in water level

6. Discussion

The carbonate coating layers at Gamsgrubenweg clearly resembles those reported by Thomazo et al. (2017) and by Liu et al. (2005). Furthermore, the presence of pustular morphologies (see Fig. 26) in some samples has also been recognized in other studies, speculated as an organic nucleus for precipitation akin to a stromatolite (Sharp et al., 1990). Nevertheless, several major new findings emerge from the present study. These are (i) the complexity of the mm-scale stratigraphy, including ripple geometries, (ii) evidence for hiatuses at the mm-scale, and (iii) the age of the deposits. Collectively, these new observations shed important new light into the evolution of the subglacial environment in the Großglockner area. Below, we consider each of these aspects in turn.

If the complexity of the stratigraphy at the mm-scale is explained by changing accommodation space beneath the glacier, what was controlling this process? In a sedimentary basin, changes in accommodation space result from rising or sinking base levels of water. In a sequence stratigraphic perspective, this could indicate sinking of a point with respect to the geoid or rising of a sea or lake level to produce relative base level rise or fall (Catuneanu, 2008). At the mm-scale, beneath the glacier, the most likely explanation for accommodation increase and loss is changes in the thickness of a subglacial meltwater film. The timescales at work here cannot be determined with certainty, but it seems likely that thicker subglacial meltwater films developed during summer months, and vice versa in the winter. Nevertheless, it is also possible that some of these changes record diurnal variation. At a much larger (m-scale), recent work in Ennstal has revealed the power of sequence stratigraphic analysis to reconstruct base level changes in a proglacial, Pleistocene lake (Le Heron et al., 2023). However, at the thin section scale - as showcased here - we are unaware of any previous attempt to utilize this methodology. As demonstrated in this study, it reveals previously undescribed sedimentary structures and stratigraphic architectures at the mm-scale.

6.1 Implications of the age of the deposits

The dates retrieved from carbonate-coating layers correspond to the Hengelo interstadial (36 000 – 38 600 BP) within the Würm glacial stage (compare with chapter 2.3 above). Correction by the calibration curve for C14 gave an absolute date of 42 350 – 41 380 (at 1-sigma confidence) for Hengelo (Vandenberghe & Van der Pflicht, 2016). This date neatly corresponds to my sample AW5, with an absolute date of 43 387 – 42 403 (1-sigma confidence).

At the beginning of the study, an age of several hundred to thousands of years for the carbonate coating layers was expected. Thus, the surprise is that the C14 analysis indicates a greater age. This raises two possibilities, namely (i) that the deposits really do represent ancient deposition or (ii) that age reflects the parent material. The place, where I had found that material, must not necessary be the place of its primary origin. Considering that such a carbonate layer is quite sensitive to chemical weathering, its exposure to atmosphere should have happened somewhat recently. The age dates require that the sample site remained covered since deposition and only recently exposed, otherwise it would have been destroyed by karstification and dissolution. Considering this, and in mind of the recent exposure of the carbonate coating layers in front of the retreating Bockkarkees, more likely explanations than an extremely old depositional event come into play. In a model proposed by Thomazo et al. (2017), parent material is eroded and transported from a source area but remains trapped within coating layers of ice (Thomazo et al., 2017). This trap area remained permanently covered with ice until a few years ago. In a few areas the material is preserved, as it is protected by erosion from the glacier in depressions. This enabled the material to stay unchanged and to survive for quite a long time period. It may be seen in Fig.5, that the orientation of the glacial abrasion is the same both at the bedrock and the carbonate layer.

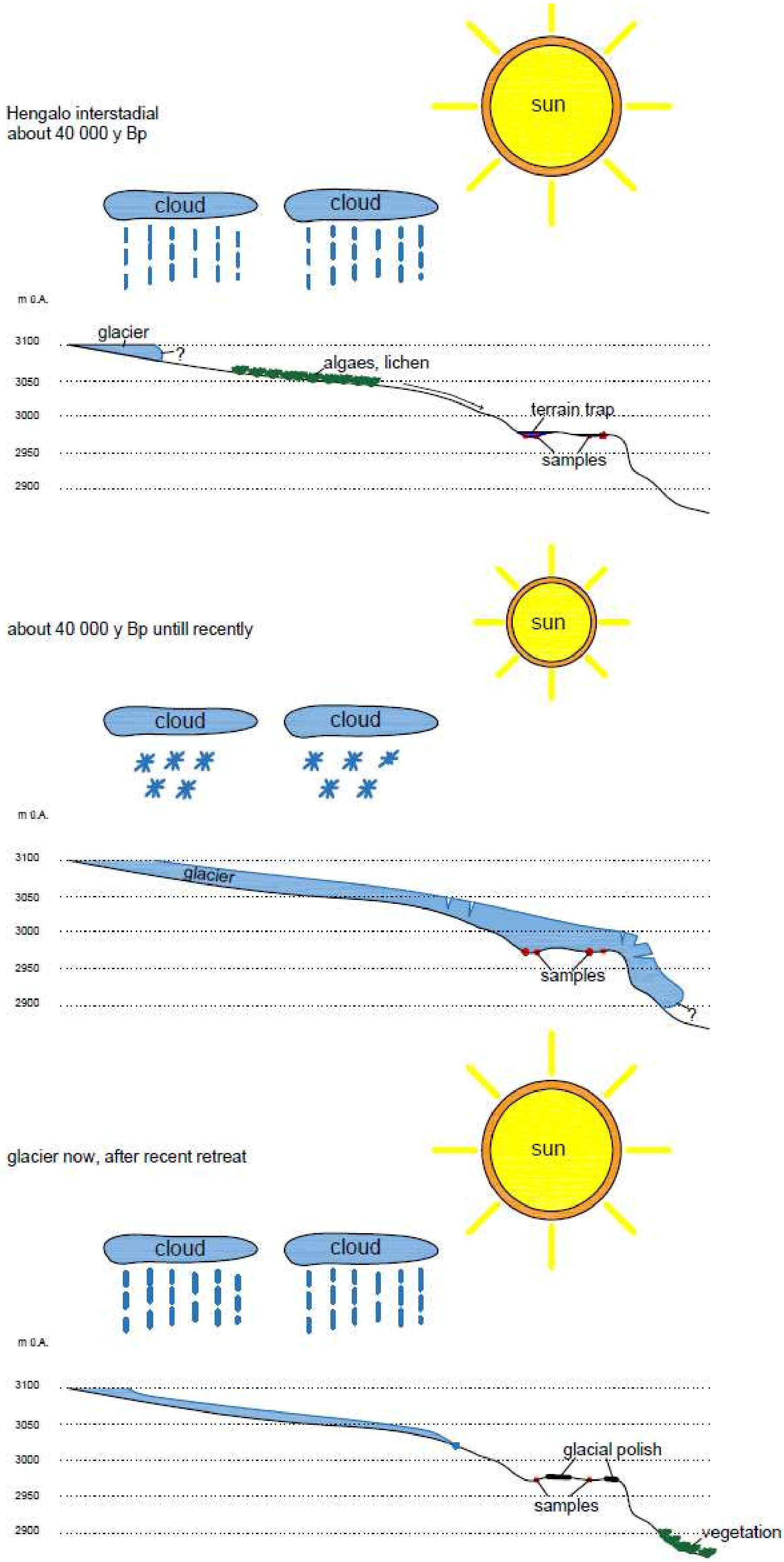

Fig. 33: Schematic representation of coating layers possible origin and development

How could my samples have been covered by ice for such a long period? The data presented by Frenzl (Zötl, 1971) give evidence that there was a period of high temperature in the climate period between 30 000 und 40 000 years before present. After that, with one single short exception around at the middle of Holocene, temperatures had always been lower than nowadays. Material might easily be washed down from their original place compare Thomazo et al., (2017) and build up these layers, visible under the microscope, in some ground depression. Glacier ice protected the deposits all the time until yet. The recent increase of temperature, causing an excessive retreat of the glacier, exposed it.

Due to the geological setting described above, there is lime mica shist at the bedrock and the surrounding area of the places where I found my samples. Therefore, I cannot exclude an admixture of Calcium carbonate from there. It is difficult to estimate its contribution to the samples, but as the layers are formed during single years the total amount of abrasion should be minor. Even if my sample contain 50% of material from old carbonate this would reduce the C14 age only for another 5700 years. That means that the sample still arise from some period of the "Göttweiger Interstadial".

Fig. 34: Carbonate layer covering the bedrock; the closer you get to rocks more recently exposed by the ice, the more frequent the deposits become (own observation)

The fine structure of my samples is typically for varves which are finely laminated sediments. The bands reflect the annual rhythm, where the darker lines represent enrichment of organic material precipitated during winter or early spring that were deposited in stagnant water. (Jürgen, 2020). Such minor pools – or maybe puddles – may easily be formed during the glaciers melting. Small lakes may be seen on the higher part of the Gamsgrubenweg even nowadays. Later, the movement of the new ice may have eroded most of this material, having left only some spots in well protected places where I found it.

Fig.35: The research area is covered with small lakes and ponds

However, the δC13 values I have obtained are much higher, than the data from Thomazo and coworkers (Thomazo, et al., 2017). Their samples turn out to be much younger in radiocarbon dating and are collected from a much deeper level (about 1760 m ü.A.). Remnants of wood and other higher plants are therefore responsible for the enrichment of C12 in their samples. My material in contrast may be the remnants from a different vegetation, algaes or lichens. Sharp and coworkers described such structures, which have a pustular morphology reminiscent to some bacterial calcites. They call it the white deposit and found unusually high δC13 values there, in a range from - 4,5‰ to + 8‰ with an $\bar{x}$=1,96 (± 5,18 sd). They explained such higher δC13 values as a result of fractionation due to photosynthetic removal of C12 by cyanobacteria (Sharp et al., 1990).

Their data are in accordance to the value of my sample AW5, 0,9‰ (± 1,0 sd). That means, the material I found was depleted of C12 by the bacterial metabolism, leaving partly enriched C13 in the substrate, whereas much of the organic material is lost and only a part of it was left.

The remaining organic carbon is responsible for the darker layers. This material was deposited during the colder time part of the year and not completely decomposed but washed downward into the terrain trap (Jürgen, 2020).

The following profile (Fig. 36) gives an idea about the investigation area showing the terrain trap mentioned above. It should be noted that this profile shows the glacier surface and not the bedrock, which forms the terrain trap at low glacier extent.

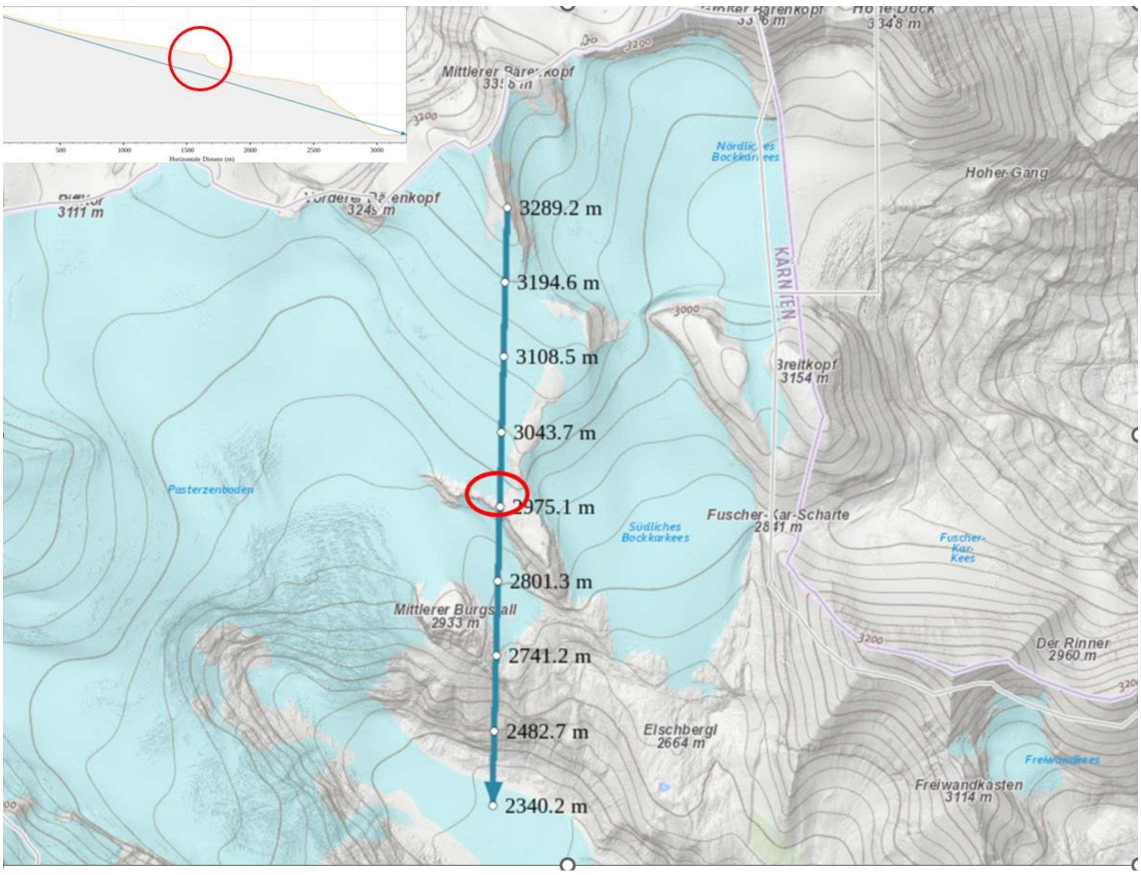

Fig: 36: Profile line through the area of interest; the red marker shows the samples location.

7.Conclusion

The carbonate coating layer sampled at an altitude of 2975 m ü.A. has been investigated by microscopy of thin sections, X-ray power diffraction and age determination by C14 including content of C13. The samples were collected from spots that had been covered by the glacier for a long period and were very recently exposed to atmosphere after glacial retreat.

- Thin section investigation reveals a complex stratigraphic architecture developed entirely within micrite.

- The fine structure of the samples contain a succession of very thin different layers, which correspond to different seasons.

- The coloration of the layers is attributed to a different proportion of organic residues

- The age determination by C14 resulted in an age of about 43 000 years BP, corresponding to the Hengelo Interstadial, an intermediate warming period during the Würm ice age.

- The material of the deposits must not necessarily be formed in situ, but was probably washed down from higher areas

8.Acknowledgements

Foremost, I thank my supervisor Univ.-Prof. Dr. Daniel Paul LE HERON for his excellent support and effort during my research. Furthermore, I would like to thank MSc. Christoph Kettler for valuable tips and information. In addition, I want to thank Dr. Jürgen Reitner (GeoSphere Austria) for his courtesy considering help with the sample and same to PhD Irka Hajdas (ETH Zürich) for the analysis of my sample.

I would also like to express big thanks to my family for their continuous emotional support and the permanent financial aid during my time period at the university.

Sincere thanks to all the people who supported me over the years.

9.References

Aharon, P. (1988). Oxygen, carbon, and U-serie isotopes of aragonites from Vestfold Hills, Antarctica. Clues to geochemical processes in subglacial environments. *Geochim, Cocmochim*(52), pp. 2321-2331.

Arnaus , F., Révillon, S., Debret, M., Revel, M., Chapron, E., Jacob , J., . . . Magny, M. (2012). Lake Bourget regional erosion patterns reconstruction reveals Holocene NW European Alps soil evolution and paleohydrology. . *Quarternary Science Reviews 51*, 81-92.

Behringer, W. (2011). *Kulturgeschichte des Klimas.* München: Deutscher Taschenbuch Verlag.

Carol, H. (1947). The formation of roches moutonnees. *Journal of Glaciology, 1*(2), pp. 57-59.

Falkenstein, F. (2012/13). Kulturwandel und Klima im 12.Jahrhunder v. Chr. Das Beispiel Kastanas in Nordgriechenland. *Offa 69/70*, pp. 505-526.

Ford, D., Fuller, P., & Drake, J. (1970). Calcite Precipitates at the Soles of Temperate Glaciers. *Nature 226*, 441-442.

Froitzheim, P. D. (2022). Vorlesungsskript Geologie der Alpen Teil 2: " Das Penninikum". Bonn, Deutschland.

Gross, H. (1956). Das Göttweiger Interstadial, ein zweiter Leithorizont der letzten Vereisung. *E & G Quartenary Sci.*(7), pp. 87-101.

Gross, H. (1960). Die Bedeutung des Göttweiger Interstadials im Ablauf der Würm-Eiszeit. *E & G - Quarternary Science Journal*(11).

Groß, H. (1968). DIe österreichische Löß-Chronologie, ihre Berichtigung und Anwendung auf das obere Pleistozän im österrreichischen Moränengebiet. *Qurtär*(19), pp. 65-80.

Hallet, B. (1976). Deposits formes by subglacial precipitation of CaCO3. *GSA Bulletin 87*, 1003-1015.

Hallet, B. (1979). Subglacial Regelation Water Film. *Journal of Glaciology, 23*(89), 321-334.

Höck, V., & Pestal, G. (1994). *153 Großglockner.* GBA.

Jürgen, E. (2020). *Das Eiszeitalter.* Berlin: Springer.

KAGIS. (2023). *KAGIS*. Retrieved from https://gis.ktn.gv.at/webgisviewer/atlas-mobile/map/Basiskarten/Amtliche%20Karten

Kenoyer, J. M. (1991). The Indus Valley Tradition of Pakistan and Western Insia. *Journal of World Prehistory, 5*, pp. 331-335.

Kers , L. (1964). Förekomster av subglacialt utfälld kalksten i solna samt i gardvik, västerbotten län. *Geologiska Föreningen i Stockholm Förhandlingnar*(86), pp. 282-310.

Kirchlechner, P. (2011). *Gletscherhydrologie der Pasterze. In Die Pasterze.* Salzburg: Anton Pustet Verlag.

Kor, P., Shaw, J., & Sharpe, D. (1991). Erosion of bedrock by subglacial meltwater, Georgien Bay, Ontario. *Canadian Jounal of Earth Sciences, 28*, 623-642.

Krainer, K. (2015). *Nationalpark Hohe Tauern Geologie.* Innsbruck-Wien: Tyrolia-Verlag.

Kurz, W., Neubauer, F., Genser, J., & Dachs, E. (1998). Alpine geodynamic evolution of passive and active contonetal margin sewuences in the tauern window (eastern alps, asutria, italy). *Geologische Rundschau 87*.

Le Heron, D. P., Kettler, C., Wawra, A., Schöpfer, M., & Grasemann, B. (2022). The sedimentological death mask of a dying glacier. *Depositional Rec., 8*, 992-1007.

Le Heron, D., Kettler , C., Davies, B., Scharfenberg, L., Eder, L., Griesmaier, G., . . . Busfield, M. (2022, Mai). Rapid geomorphological and sedimentological changes at a modern Alpine ice margin: lessons from Gepatsch Glacier, Tirol, Austria. *Journal of Geological Society, 179*(3).

Le Heron, D., Vandyk, T., Hongwei, K., Liu, Y., Chen, X., Wang, Y., . . . Shields , G. (2019). Bird´s-eye viw of an Ediacaran subglacial landscape. *Geology, 47*, 705-709.

Lieb, G., & Kellerer-Pirklbauer, A. (2018). *Die Pasterze, Österreich größter Gletscher, und seine lange Messreihe in einer Ära massiven Gletscherschwundes in Gletscher in Wandel.* Berlin: Springer Verlag.

Lipar , M., Martin-Pérez, A., Ticar, J., Pavsek, M., Gabrovec, M., Hrvatin , M., . . . Ferk, M. (2021). Sublaglacial carbonate deposits as a potential proxy for a glacier`s former presence. *The Cryosphere 15*, 17-30.

Liu, G., Luo, R., Cao, J., & Cui, Z. (2005). Process and environmental significance of the subglacial chemical deposits in Tianshan Mountains. *Sciene in China Ser. D Earth Sciences*(48/9), pp. 1470-1478.

Nicolussi, K. (2011). *Gletschergeschichte der Pasterze In. Die Pasterze.* Salzburg: Anton Pustet Verlag.

Paszkowicz, W. (2006). Ninety Years of Powder Diffraction: from Birth to Maturity. *Synchrotron Radiation in Natural Science, 1-2*(Vol 5).

Qayyum , F., Catuneanu, O., & De Groot, P. (2014). Historical developments in Wheeler diagramm and future directions. *Basin Research, 26*, 1-15.

Qayyum, F., Betzler, C., & Catuneanu, O. (2017). The Wheeler diagramm, flattening theory, and time. *Marine and Petroleum Geology, 86*, 1417-1430.

Refsnider, K., Miller, G., Foget, M., Frechette, B., Bowden, R., Andrews, J., & Farmer, G. (2017). Subglacially precipitated carbonates record geochemical interactions and pollen preservation at the base of the Laurentide Ice Sheet of central Baffin island, eastern Canadian Arctic. *Q.Res*(81), pp. 94-105.

Ross-Macdonald, M. (1971). *Hölzerne Schiffe, eiserne Männer. Part 3: Island und Grönland. In: Aufbruch ins Unbekannte.* Gütersloh: Prisma Verlag.

Samuelsson, L. (1964). Nya Fynd av Subglacialt Bildade Kalkstenar. *Geologiska Föreningen i. Stockholm Förhandlingnar*(85), pp. 414-427.

Schrenner, E. (2011). *Gletscherdynamik - Bewegung und Fließgrschwindigkeit kalter, temperierter und polythermaler Gletscher.* München: Grin Verlag.

Sharp, M., Tison, J.-L., & Fierens, G. (1990). Geochemistry of subglacial calcites: implications for the hydrology of the basal water film. *Arctic and Alpine Research 22*, 141-152.

Sharp, M., Tisot, J.-L., & Fierens, G. (1990). Geochemistry of Subglacial Calcites: Implications for the Hydrology of the Basal Water Film. *Arctic and Alpine Research, 22/2*, pp. 141-152.

Siman-Tov, S., Stock, G. M., Brodsky, E. E., & White, J. C. (2017, November). The coating layer of glacial polish. *Geology*, pp. 987-990.

Soden, W. (1961). *Sumer, Babylon und Hethiter bis zur Mitte des Zweiten Jahrtausends v. Chr. In: Weltgeschichte, Bd.1 Frühe Hochulturen.* Gütersloh: Prisma Verlag.

Strauß, A., & Strauß, A. (2020, 3). *Alpenverein*. Retrieved from https://www.alpenverein-muenchen-oberland.de/uploads/images/tSpR9pbc0DxtdU1R4NAHIg/gamsgrubenweg.pdf

Stüwe, K., & Homberger, R. (2015). *Die Geologie der Alpen aus der Luft.* Gnas: Weishaupt Verlag.

Thomazo, C., Buonchristiani, J.-F., Vennin, E., Pellenard, P., Cocquerez, T., Mugnier, J. L., & Gerard, E. (2017, September). Geochemical Processes Leading to the Precipitation of Subglacial Carbonate Crusts at Bossons Glacier, Mont Blanc Massif (French Alps). *Frontier in Earth Science*(Volume 5), pp. 1-16.

Tintor, W. (1993). Die Kleingletscher der Julischen Alpen. *Carinthia II 183*, 405-424.

Treydte, K., Esper, J., & Gärtner, H. (2004). Stabile Isotope in der Dendroklimatologie. *Schweiz. Z. Forstwes. 155/6*, pp. 222-232.

Treydte, K., Gärtner, H., & Esper, J. (2004). Stabile Isotope in der Dendroklimatologie. *Schweiz.Z.Forstwesen 155*, 222-232.

Vandenberghe, J., & Van der Pflicht, J. (2016). The age of the Hengelo interstadial revisited. *Quaternary Geochronology*, pp. 21-28.

Wernick, R. (1980). *Die Wikinger.* Amsterdam: Time Life Bücher.

Wilson, J. (1961). *Ägypten. In: Weltgeschichte, Bd.1 Frühe Hochkulturen.* Gütersloh: Prisma Verlag.

Woldstedt, P. (1958). Eine neue Kurve der Würm-Eiszeit. *E & G Quarternary Science Journal*(07), pp. 78-86.

Zagwijn, W., & Paepe, R. H. (1968, Oktober 31). Die Stratigraphie der wecihselzeitlichen Ablagerung der Niederlande und Belgiens. *Eiszeitalter und Gegenwart, 19*, pp. 129-146.

Zötl, J. (1971). Isotopenmessung in der Hydrogeographie als Hilfsmittel zur Untersuchung der Klimaschwankungen in der Spät- und Nacheiszeit. *Mitt. naturwiss. Ver. Steiermark*, pp. 197-198.